Title: A bacterium that degrades and assimilates poly(ethylene terephthalate)

Authors: Shosuke Yoshida[1,2†], Kazumi Hiraga[1], Toshihiko Takehana[3], Ikuo Taniguchi[4], Hironao Yamaji[1], Yasuhito Maeda[5], Kiyotsuna Toyohara[5], Kenji Miyamoto[2]*, Yoshiharu Kimura[4], & Kohei Oda[1]*

Affiliations:

[1]Department of Applied Biology, Faculty of Textile Science, Kyoto Institute of Technology, Matsugasaki, Sakyo-ku, Kyoto 606-8585, Japan

[2]Department of Biosciences and Informatics, Keio University, 3-14-1 Hiyoshi, Kohoku-ku, Yokohama, Kanagawa 223-8522, Japan

[3]Life Science Materials Laboratory, ADEKA Corporation, 7-2-34 Higashiogu, Arakawa-ku, Tokyo 116-8553, Japan

[4]Department of Polymer Science, Faculty of Textile Science, Kyoto Institute of Technology, Matsugasaki, Sakyo-ku, Kyoto 606-8585, Japan

[5]Ecology-Related Material Group Innovation Research Institute, Teijin Ltd., Hinode-cho 2-1, Iwakuni, Yamaguchi 740-8511, Japan

[†]Current address: Department of Polymer Chemistry, Graduate School of Engineering, Kyoto University, Nishikyo-ku, Kyoto 615-8530, Japan

*Correspondence to: K.M. (kmiyamoto@bio.keio.ac.jp) or K.O. (bika@kit.ac.jp).

Abstract: Poly(ethylene terephthalate) (PET) is used extensively worldwide in plastic products, and its accumulation in the environment has become a global concern. Because the ability to enzymatically degrade PET for microbial growth has been limited to a few fungal species, biodegradation is not yet a viable remediation or recycling strategy. By screening natural microbial communities exposed to PET in the environment, we isolated a novel bacterium, *Ideonella sakaiensis* 201-F6, that is able to utilize PET as its major energy and carbon source. When grown on PET, this strain produces two enzymes capable of hydrolyzing PET and the reaction intermediate, mono(2-hydroxyethyl) terephthalic acid (MHET). Both enzymes are required to enzymatically convert PET efficiently into its two environmentally benign monomers, terephthalic acid and ethylene glycol.

Main Text: Plastics with desirable properties such as durability, plasticity, and/or transparency have been industrialized over the last century and widely incorporated into countless consumer products (*1*). Many of these products are remarkably persistent in the environment due to the absence or low activity of catabolic enzymes that might otherwise break down their plastic constituents. In particular, polyesters containing a high ratio of aromatic components, such as poly(ethylene terephthalate) (PET), are chemically inert, resulting in resistance to microbial degradation (*2, 3*). Approximately 56 million tons of PET was produced worldwide in 2013 alone, prompting further industrial production of its monomers, terephthalic acid (TPA) and ethylene glycol (EG), both of which are derived from raw petroleum. Large quantities of PET have been introduced into the environment through its production and disposal, resulting in the accumulation of PET in environments across the globe (*4*).

There are very few reports on the biological degradation of PET or its utilization to support microbial growth. Rare examples include members of the filamentous fungi *Fusarium oxysporum and F. solani,* that can grow on a mineral medium containing PET yarns [although no growth levels were specified] (*5, 6*). Once identified, microorganisms having enzymatic machinery to degrade PET could serve as an environmental remediation strategy as well as a degradation/fermentation platform for biological recycling of PET waste products.

We collected 250 PET debris-contaminated environmental samples including sediment, soil, wastewater, and activated sludge from a PET-bottle recycling site (*7*). Using these samples, we screened for microorganisms that could use low crystallinity (1.9%) PET film as the major carbon source for growth. One sediment sample contained a distinct microbial consortium that formed on the PET film upon culturing (Fig. 1A) and induced morphological change of the PET film (Fig. 1B). Microscopy revealed that the consortium on the film, termed "No. 46", contained a mixture of bacteria, yeast-like cells, and protozoa, whereas the culture fluid was almost transparent (Fig. 1A). This consortium degraded the PET film surface (Fig. S1) at a rate of 0.13 mg/cm^2/day at 30°C (Fig. 1C). Seventy-five percent of the degraded PET film carbon was catabolized into CO_2 at 28°C (Fig. S2).

Using limiting dilutions of consortium No. 46 that were cultured with PET film to enrich for microorganisms nutritionally dependent on PET, we successfully isolated a bacterium capable of degrading and assimilating PET. The strain represents a novel species of the genus *Ideonella*, for which we propose the name *Ideonella sakaiensis* 201-F6 (NCBI taxonomy database, ID: 1547922). In addition to being found in the culture fluid, cells were observed on the film (Fig. 1D) and appeared to be connected to each other by appendages (Fig. 1E). Shorter appendages were observed between the cells and the film and these might assist delivery of

secreted enzymes into the film (Fig. 1, D and F). The PET film was damaged extensively (Fig. 1G) and almost completely degraded after 6 weeks at 30°C (Fig. 1H). In the course of subculturing No. 46, we found a consortium that lost its PET degradation capability. This consortium lacked *I. sakaiensis* (Fig. S3), indicating that this strain is functionally involved in PET degradation within the consortium.

There are currently very few examples of esterases, lipases, or cutinases that are capable of hydrolyzing PET (*8, 9*). To explore the genes involved in PET hydrolysis in *I. sakaiensis* 201-F6, we assembled a draft sequence of its genome (Table S1). One gene (ISF6_4831) was identified that encodes a putative lipase sharing 51% amino acid sequence identity and catalytic residues with a hydrolase from *Thermobifida fusca* (TfH) (Table S2 and Fig. S4), and which exhibits PET-hydrolytic activity (*10*). We purified the corresponding recombinant *I. sakaiensis* proteins (Fig. S5) and incubated them with PET film at 30°C for 18 h. Prominent pitting developed on the film surface (Fig. 2A). Mono(2-hydroxyethyl) terephthalic acid (MHET) was the major product released by the recombinant protein, together with minor amounts of TPA and bis(2-hydroxyethyl) TPA (BHET) (Fig. 2B). These results suggested that the ISF6_4831 protein hydrolyzes PET. This protein also hydrolyzed BHET to yield MHET with no further decomposition.

We compared the activity of the ISF6_4831 protein to that of three evolutionarily divergent PET-hydrolytic enzymes identified from a phylogenetic tree constructed using published enzymes (Fig. 2C and Table S2). We purified TfH from a thermophilic actinomycete (*10*), LC-cutinase (LCC) from a compost metagenome (*11*), and *F. solani* cutinase (FsC) from a fungus (*12*) (Fig. S5), and measured their activities against *para*-nitrophenol (*p*NP)-linked aliphatic esters, PET film, and BHET at 30°C, pH 7.0. For *p*NP-aliphatic esters, that are

preferred by lipases and cutinases, the activity of the ISF6_4831 protein was lower than that of TfH, LCC, and FsC (Fig. 2D). The activity of the ISF6_4831 protein against the PET film, however, was 120-, 5.5-, and 88-fold higher than that of TfH, LCC, and FsC, respectively. A similar trend was observed for BHET (Fig. 2D). The catalytic preference of the ISF6_4831 protein for PET film versus *p*NP-aliphatic esters was also substantially higher than that of TfH, LCC, and FsC (380-, 48-, and 400-fold on average, respectively) (Fig. 2D). Thus, the ISF6_4831 protein preferred PET to aliphatic esters, compared with the other enzymes, leading to its designation as a PET hydrolase (PETase).

PETase was also more active than TfH, LCC, and FsC against commercial bottle-derived PET, which is highly crystallized (Fig. 2E), even though the densely packed structure of highly crystallized PET greatly reduces enzymatic hydrolysis of its ester linkages (*9, 13*). PETase was somewhat heat-labile, but remarkably more active against PET film at low temperatures than TfH, LCC, and FsC (Fig. 2F). Enzymatic degradation of polyesters is controlled mainly by their chain mobility (*14*). Flexibility of the polyester chain decreases as the glass transition temperature (T_g) increases (*9*). The T_g of PET is around 75°C; i.e. the polyester chain of PET is in a glassy state at moderate temperatures appropriate for mesophilic enzyme reactions. The substrate specificity of PETase, and its prominent hydrolytic activity for PET in a glassy state, would be critical to sustaining growth of this strain on PET in most environments where PET products exist.

I. sakaiensis adheres to PET (Fig. 1D–F) and secretes PETase to target this material. We compared the PET hydrolytic activity of PETase with that of the other three PET hydrolytic enzymes (Fig. S7). The activity ratios of PETase versus the other enzymes decreased as the enzyme concentrations increased, indicating that PETase efficiently hydrolyzed PET with less

enzyme diffusion into the aqueous phase and/or plastic vessels used for the reaction. PETase lacks apparent substrate-binding motif(s) such as carbohydrate binding modules generally observed in glycoside hydrolases. Therefore, without the 3D structure of PETase, the exact binding mechanism is unknown.

MHET, the product of PETase-mediated hydrolysis of BHET and PET, was an extremely minor component in the supernatant of *I. sakaiensis* cultured on PET film (Fig. S8), indicating rapid MHET metabolism. Several PET hydrolytic enzymes have been confirmed to hydrolyze MHET (Table S2). To identify enzyme(s) responsible for PET degradation in *I. sakaiensis* cultures, we sequenced transcriptomes of *I. sakaiensis* cells growing on maltose, disodium terephthalate (TPA-Na), BHET, or PET film (Fig. S9) (RNA-Seq, Table S3). The catabolic genes for TPA and the metabolite protocatechuic acid (PCA) were upregulated dramatically when cells were cultured on TPA-Na, BHET, or PET film. This was in contrast to genes for the catabolism of maltose (Fig. 3A), which involves a pathway distinct from the degradation of TPA and EG. This indicates efficient metabolism of TPA by *I. sakaiensis*. Interestingly, the transcript level of the PETase gene during growth on PET film was the highest among all analyzed coding sequences (Table S4), and it was 15-, 31-, and 41-fold higher than when bacteria were grown on maltose, TPA-Na, and BHET, respectively. This suggests that PET film itself, and/or some degradation products other than TPA, EG, MHET, and BHET, induce(s) the expression of PETase.

The expression levels of the PETase gene in the four different media were similar to those of another gene, ISF6_0224 (Fig. S10), indicating similar regulation. ISF6_0224 is located adjacent to the TPA degradation gene cluster (Fig. S11). The ISF6_0224 protein sequence matches those of the tannase family, which is known to hydrolyze the ester linkage of aromatic

compounds such as gallic acid esters, ferulic saccharides, and chlorogenic acids. The catalytic triad residues, and two cysteine residues found uniquely in this family (*15*), are completely conserved in the ISF6_0224 protein (Fig. S12). Purified recombinant ISF6_0224 protein (Fig. S5) efficiently hydrolyzed MHET with a turnover rate (k_{cat}) of 31 $\pm$ 0.8 sec^{-1} and a K_m of 7.3 $\pm$ 0.6 μM (Table 1), but did not show any activity against PET, BHET, *p*NP-aliphatic esters, or typical aromatic ester compounds catalyzed by the tannase family enzymes (Table 1). ISF6_0224 is non-homologous to six known MHET-hydrolytic enzymes that also hydrolyze PET and *p*NP-aliphatic esters (Table S2). These results strongly suggest that the ISF6_0224 protein is responsible for the conversion of MHET to TPA and EG in *I. sakaiensis*. The enzyme was thus designated MHET hydrolase (MHETase).

We attempted to determine how the metabolism of PET (Fig. 3B) evolved by searching for other organisms capable of metabolizing this compound using the Integr8 fully sequenced genome database (*16*). However, we were unable to find other organisms harboring a set of gene homologs of signature enzymes for PET metabolism (PETase, MHETase, TPA dioxygenase, and PCA dioxygenase) (Fig. S13). In contrast, among the 92 microorganisms harboring MHETase homolog(s), 33 had homologs of both TPA and PCA dioxygenases. This suggests that a genomic basis to support the metabolism of MHET analogues was established much earlier than when ancestral PETase proteins were incorporated into the pathway. PET enrichment in the sampling site and enrichment culture potentially promoted the selection of a bacterium that might have obtained the set of genes through lateral gene transfer. A limited number of mutations in a hydrolase, such as PET hydrolytic cutinase, that inherently targets the natural aliphatic polymer cutin, may have resulted in enhanced selectivity for PET.

References and Notes:

1. V. Sinha, M. R. Patel, J. V. Patel, Pet waste management by chemical recycling: A review. *J. Polym. Environ.* **18**, 8–25 (2010).
2. R. J. Müller, I. Kleeberg, W. D. Deckwer, Biodegradation of polyesters containing aromatic constituents. *J. Biotechnol.* **86**, 87–95 (2001).
3. D. Kint, S. Munoz-Guerra, A review on the potential biodegradability of poly(ethylene terephthalate). *Polym. Int.* **48**, 346–352 (1999).
4. Eds. L. Neufeld, F. Stassen, R. Sheppard, T. Gilman, The new plastics economy: Rethinking the future of plastics. *World Economic Forum* (2016). http://www3.weforum.org/docs/WEF_The_New_Plastics_Economy.pdf
5. T. Nimchua, H. Punnapayak, W. Zimmermann, Comparison of the hydrolysis of polyethylene terephthalate fibers by a hydrolase from *Fusarium oxysporum* LCH I and *Fusarium solani* f. sp. *pisi*. *Biotechnol. J.* **2**, 361-364 (2007).
6. T. Nimchua, D. E. Eveleigh, U. Sangwatanaroj, H. Punnapayak, Screening of tropical fungi producing polyethylene terephthalate-hydrolyzing enzyme for fabric modification. *J. Ind. Microbiol. Biot.* **35**, 843-850 (2008).
7. Materials and methods are available as supplementary materials on *Science* Online.
8. D. Ribitsch *et al.*, Characterization of a new cutinase from *Thermobifida alba* for PET-surface hydrolysis. *Biocatal. Biotransform.* **30**, 2–9 (2012).
9. W. Zimmermann, S. Billig, Enzymes for the biofunctionalization of poly(ethylene terephthalate). *Adv. Biochem. Eng. Biotechnol.* **125**, 97–120 (2011).
10. R. J. Müller, H. Schrader, J. Profe, K. Dresler, W. D. Deckwer, Enzymatic degradation of poly(ethylene terephthalate): Rapid hydrolyse using a hydrolase from *T. fusca*. *Macromol. Rapid Commun.* **26**, 1400–1405 (2005).
11. S. Sulaiman *et al.*, Isolation of a novel cutinase homolog with polyethylene terephthalate-degrading activity from leaf-branch compost by using a metagenomic approach. *Appl. Environ. Microbiol.* **78**, 1556–1562 (2012).
12. C. M. Silva *et al.*, Cutinase - A new tool for biomodification of synthetic fibers. *J. Polym. Sci. Part A: Polym. Chem.* **43**, 2448–2450 (2005).
13. M. A. M. E. Vertommen, V. A. Nierstrasz, M. van der Veer, M. M. C. G. Warmoeskerken, Enzymatic surface modification of poly(ethylene terephthalate). *J. Biotechnol.* **120**, 376–386 (2005).
14. E. Marten, R. J. Müller, W. D. Deckwer, Studies on the enzymatic hydrolysis of polyesters. II. Aliphatic-aromatic copolyesters. *Polym. Degrad. Stab.* **88**, 371–381 (2005).
15. K. Suzuki *et al.*, Crystal structure of a feruloyl esterase belonging to the tannase family: a disulfide bond near a catalytic triad. *Proteins* **82**, 2857-2867 (2014).
16. P. Kersey *et al.*, Integr8 and Genome Reviews: integrated views of complete genomes and proteomes. *Nucleic Acids Res.* **33**, D297–302 (2005).
17. M. Hosaka *et al.*, Novel tripartite aromatic acid transporter essential for terephthalate uptake in *Comamonas* sp. strain E6. *Appl. Environ. Microbiol.* **79**, 6148–6155 (2013).

Acknowledgements: We are grateful to Y. Horiuchi, M. Uemura, T. Kawai, K. Sasage, and S. Hase for research assistance. We thank D. Dodd, H. Atomi, T. Nakayama, and A. Wlodawer for comments on this manuscript. This study was supported by a grant-in-aid for scientific research (nos. 24780078 and 26850053 to S.Y.) and the Noda Institute for Scientific Research (to S.Y.). The reported nucleotide sequence data, including assembly and annotation, have been deposited at the DDBJ/EMBL/GenBank databases under the accession numbers BBYR01000001-BBYR01000227. All other data are reported in the Supplementary Materials. The reported strain *Ideonella sakaiensis* 201-F6^{T} was deposited at NITE Biological Resource Center (NBRC) as strain NBRC 110686^{T}, and at Thailand Institute of Scientific and Technological Research (TISTR) as strain TISTR 2288^{T}.

Supplementary Materials:

www.sciencemag.org

Materials and Methods

Text S1 and S2

Tables S1 to S5

Figures S1 to S14

Full Reference List

220

Table 1. Kinetic parameters of MHETase[a].

Substrate	k_{cat} (s^{-1})	K_m (μM)
MHET	31 ± 0.8[b]	7.3 ± 0.6[b]
PET film	ND[c]	
BHET	0.10 ± 0.004[d]	
*p*NP-aliphatic esters (*p*NP-acetate, *p*NP-butyrate)	ND	
Aromatic esters (ethyl gallate, ethyl ferulate, chlorogenic acid hydrate)	ND	

[a]Determined in pH 7.0 buffer at 30°C.
[b]Data are shown as means ± SEs based on a nonlinear regression model.
[c]ND, not detected; activity was below the detection limit of the assay.
[d]The reported k_{cat} is the apparent k_{cat} determined with 0.9 mM BHET. Data are shown as means ± SEs from three independent experiments.
Because the enzymatic PET hydrolysis involves a heterogeneous reaction, Michaelis–Menten kinetics were not applied to PETase.

221

222

223 **Figure legends:**

224

225 **Fig. 1. Microbial growth on PET.** (**A**–**C**) PET film (60 mg, 20 × 15 × 0.2 mm) degradation by
226 microbial consortium No. 46 in 10 mL of MLE medium at 30°C. Medium was changed biweekly.
227 (**A**) Growth of No. 46 on PET film after 20 days. (**B**) SEM image of degraded PET film after 70
228 days. Inset, intact PET film. Bar, 0.5 mm. (**C**) Time course of PET film degradation by No. 46.
229 (**D**–**H**) PET film degradation by *I. sakaiensis* 201-F6 in YSV medium at 30°C with a weekly
230 medium change. (**D**–**F**) SEM images of *I. sakaiensis* cells grown on PET film for 60 h. Bars, 1
231 μm. Arrow heads in the left panel of (**D**) indicate contact points of cell appendages and PET film
232 surface. Magnifications are shown in the right panel. Arrows in (**F**) indicate appendages between
233 the cell and the PET film surface. (**G**) SEM image of a degraded PET film surface after washing
234 out adherent cells. Inset, intact PET film. Bar, 1 μm. (**H**) Time course of PET film degradation
235 by *I. sakaiensis*.

236

237 **Fig. 2. ISF6_4831 protein is a PET hydrolase (PETase).** (**A**–**B**) Effect of PETase on PET film.
238 PET film (⌀6 mm) was incubated with 50 nM PETase in pH 7.0 buffer for 18 h at 30°C. (**A**)
239 SEM image of the treated PET film surface. Inset, intact PET film. Bar, 5 μm. (**B**) HPLC
240 spectrum of the products released from the PET film. (**C**) Unrooted phylogenetic tree of known
241 PET hydrolytic enzymes. The GenBank or PDB accession numbers (source of protein) are
242 shown. Bar, 0.1 amino acid substitutions per single site. Bootstrap values are shown at the
243 branch points. (**D**) Substrate specificity of four phylogenetically distinct PET hydrolytic enzymes.
244 All reactions were performed in pH 7.0 buffer at 30°C. PET film was incubated with 50 nM
245 enzyme for 18 h. (**E**) Activity of the PET hydrolytic enzymes for highly crystallized PET

(hcPET). hcPET (⌀6 mm) was incubated with 50 nM PETase, or 200 nM TfH, LCC, or FsC, in pH 9.0 Bicine-NaOH buffer for 18 h at 30°C. (**F**) Effect of temperature on enzymatic PET film hydrolysis. PET film (⌀6 mm) was incubated with 50 nM PETase, or 200 nM TfH, LCC, or FsC, in pH 9.0 Bicine-NaOH buffer for 1 h. For better detection of the released products in (E) and (F), the pH and enzyme concentration were determined based on the results shown in Figs. S6 and S7, respectively. Error bars in (**D–F**) indicate SE (n≥3).

Fig. 3. PET metabolism by *Ideonella sakaiensis*. (**A**) Transcript levels of selected genes when grown on TPA-Na, PET film, or BHET, relative to those when grown on maltose. Two-sided *p*-values were derived from Baggerly's test of the differences between the means for two independent RNA-Seq experiments (*$p < 0.05$; **$p < 0.01$). (**B**) Predicted *I. sakaiensis* PET degradation pathway. First, the cellular localization of PETase and MHETase was predicted (Text S1). Extracellular PETase hydrolyzes PET to produce MHET (major product) and TPA. MHETase, a predicted lipoprotein, hydrolyzes MHET to TPA and EG. TPA is incorporated through the TPA transporter (TPATP) (*17*) and catabolized by TPA 1,2-dioxygenase (TPADO), followed by 1,2-dihydroxy-3,5-cyclohexadiene-1,4-dicarboxylate dehydrogenase (DCDDH). The resultant PCA is ring-cleaved by PCA 3,4-dioxygenase (Pca34). The predicted TPA degradation pathway is further described in Text S2.

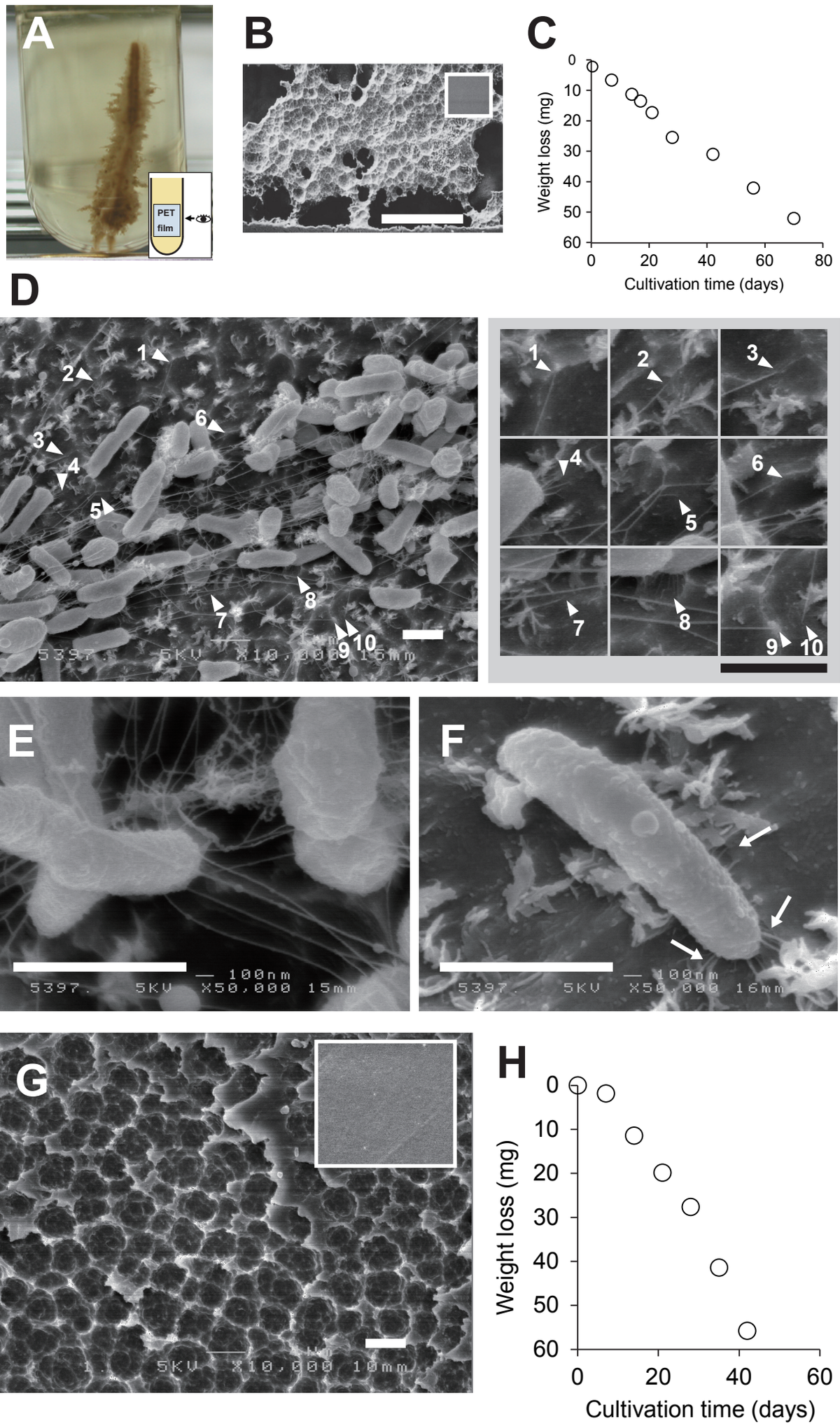

Fig. 1 Yoshida *et al*.

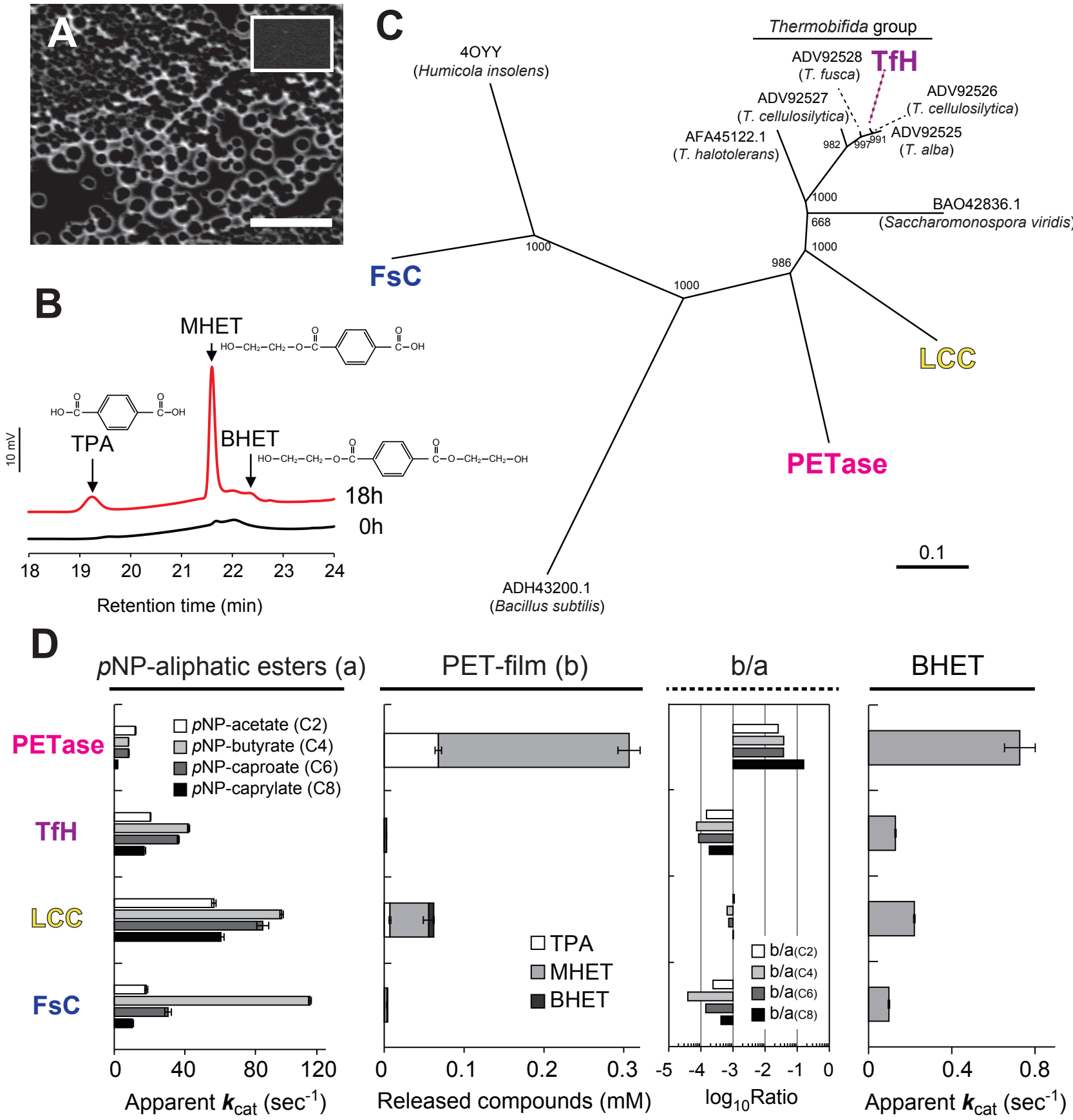

Fig. 2 Yoshida *et al*.

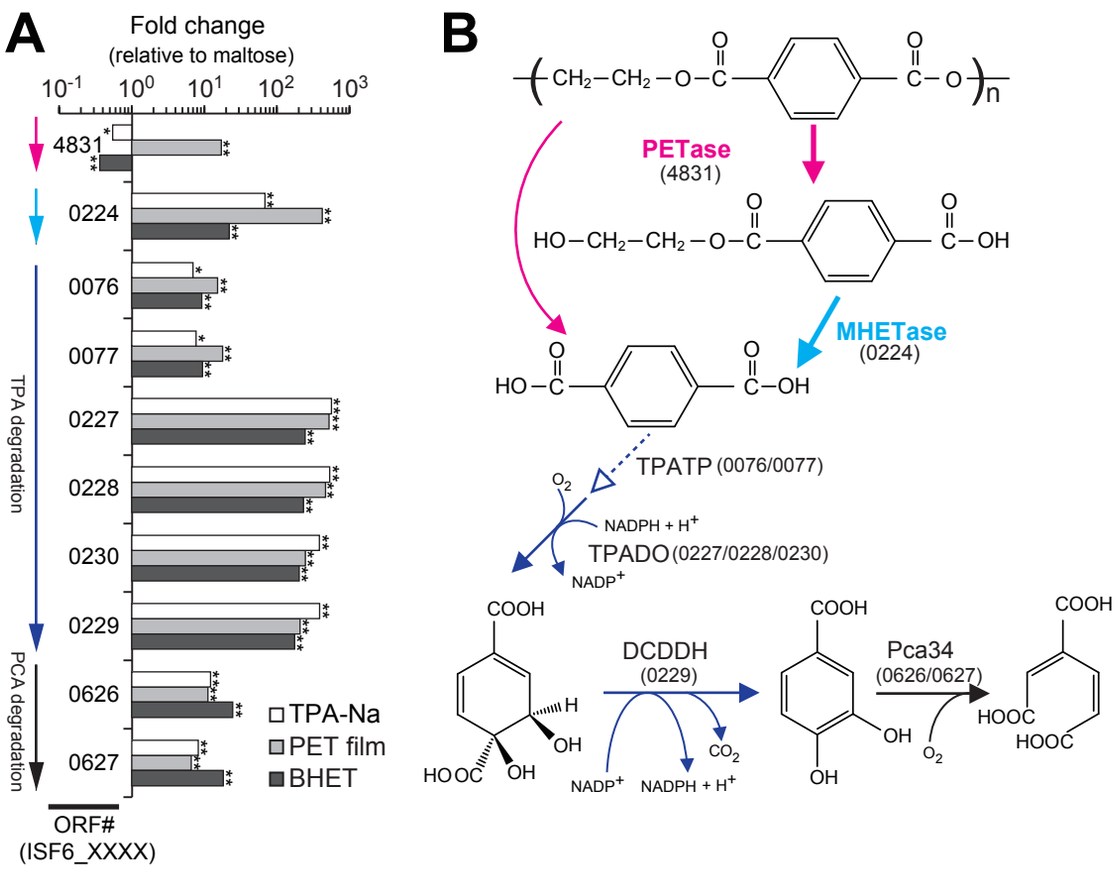

Fig. 3 Yoshida *et al*.

Supplementary Materials for

A bacterium that degrades and assimilates poly(ethylene terephthalate)

S. Yoshida, K. Hiraga, T. Takehana, I. Taniguchi, H. Yamaji, Y. Maeda, K. Toyohara, K. Miyamoto*, Y. Kimura, K. Oda*

*Correspondence to: K.M. (kmiyamoto@bio.keio.ac.jp) or K.O. (bika@kit.ac.jp).

This file includes:

Materials and Methods:

Screening. Two hundred fifty PET-contaminated (for approximately five years) environmental samples (sediment, soil, waste water, and activated sludge) were collected at a yard of PET bottle-recycling factory in Sakai city, Osaka, Japan. They were taken from 2~3 cm below the water level or from land surface. Approximately 1 g of the samples was individually cultivated in a test tube (⌀18 × 180 mm) containing 10 mL of 0.05% yeast extract, 0.2% ammonium sulfate, and 1% trace elements (0.1% $FeSO_4 \cdot 7H_2O$, 0.1% $MgSO_4 \cdot 7H_2O$, 0.01% $CuSO_4 \cdot 5H_2O$, 0.01% $MnSO_4 \cdot 5H_2O$, and 0.01% $ZnSO_4 \cdot 7H_2O$) in 10 mM phosphate buffer (pH 7.0) with low-crystallinity PET thin film (PET film) (ca. 60 mg, 20 × 15 × 0.2 mm, Mw: 45×10^3, Mw/Mn: 1.9, T_g: 77°C, T_m: 255°C, crystallinity: 1.9%, density: 1.3378 g/cm^3). The PET film was sterilized in 70% ethanol and dried in sterile air before being placed in the test tube. The tube was shaken at 300 strokes/min at 30°C. Modified lettuce and egg (MLE) medium containing 0.15% dried lettuce extract, 0.15% egg extract, 0.2% ammonium sulfate, and 1% of the trace elements in 10 mM phosphate buffer (pH 7.0) was used for stable culture of No. 46.

Quantification of CO_2 generation. Consortium No. 46 was cultivated for 15 days in 270 mL of MLE medium in a 300 mL flask containing 4 PET films (1.4 × 15 cm) at 28°C with constant aeration (20 mL/min) and stirring. The generated CO_2 was entrapped in Ascarite and the weight was measured to calculate the absorbed CO_2. The device was constructed according to JIS K6951. After cultivation, the biofilm-like materials and treated PET films were separated from the medium. The medium was centrifuged at 8,000 rpm for 20 min. The total organic carbon

41 (TOC) contents of the supernatant and precipitate were analyzed using a standard method (JIS
42 K0102-22). The conversion rate from PET to CO_2 (R) was calculated as follows.
43
44 $$\mathrm{R}\ (\%) = \frac{\mathrm{CO_2\ (PET+)} - \mathrm{CO_2\ (PET-)}}{\text{carbon weight of the degraded PET film}} \times 100$$
45
46 where CO_2 (PET+) and CO_2 (PET−) indicate the carbon weight of generated CO_2 cultivated in
47 the presence and absence of PET, respectively.
48
49 **^{1}H-NMR spectroscopy.** PET film was dissolved in a small volume of a mixture of deuterated
50 chloroform and trifluoroacetic acid (4:1 v/v). The resultant solution was subjected to ^{1}H-NMR
51 spectroscopy using a Varian XL-200 NMR spectrometer (200 MHz).
52
53 **Gel permeation chromatography (GPC).** PET film was dissolved in 1,1,1,3,3,3-hexafluoro-2-
54 propanol (HFIP) containing 1 mM sodium trifluoroacetate at a concentration of 5 mg/mL and
55 was analyzed by GPC using a Shimadzu (Kyoto, Japan) GPC system with a HFIP-803 gel
56 column (7.5 × 300 mm) from Shodex (Tokyo, Japan). HFIP containing 1 mM sodium
57 trifluoroacetate was used as the eluent at a flow rate of 0.6 mL/min at 35°C. The molecular
58 weight was calibrated with poly(methyl methacrylate) standards (GL Science, Tokyo, Japan).
59
60 **Isolation of *Ideonella sakaiensis* 201-F6.** No. 46 was serially diluted using the most probable
61 number approach (*18*) in prototypical yeast extract–sodium carbonate–vitamins (pYSV)
62 medium: 0.01% yeast extract, 0.02% sodium hydrogen carbonate, 0.1% ammonium sulfate,
63 0.01% calcium carbonate, 0.1% vitamin mixture (0.05% thiamine-HCl, 0.05% niacin, 0.03% *p*-

aminobenzoic acid, 0.01% pyridoxal-HCl, 0.01% pantothenate, 0.005% biotin, and 0.05% vitamin B12), and 1% of the trace elements in 10 mM phosphate buffer (pH 7.0). Each diluted sample was cultured with a PET film (⌀6 mm) in a well of a 96-well plate at 30°C for 6 days. PET degradation activity was estimated visually on the basis of change of transparency of the film due to the degradation. From the positive samples, the sample that was the most diluted at the start of cultivation was used in the next round of the assay. This cycle was repeated to concentrate PET-lytic microorganisms. To monitor microbial members in the culture, the 16S rDNA V3–V5 region was amplified by PCR from genomic DNA extracted from the culture using a pair of bacterial 16S rDNA specific primers (forward, 5′-CGCCCGCCGCGCCCCGCGCCCGTCCCGCCGCCCCCGCCCGCCTACGGGAGGCAGCAG-3′; reverse, 5′-CCCCGTCAATTCCTTTGAGTTT-3′, nucleotides corresponding to GC clump are underlined), and was analyzed by denaturing gradient gel electrophoresis (DGGE) (*19*). The culture displaying one band in the PCR-DGGE was spread on a 0.5% soft agar plate containing pYSV medium, and a resultant single colony was selected.

Growth of *Ideonella sakaiensis* on PET film. *I. sakaiensis* was grown on 1.5% agarose NBRC 802 medium containing 1.0% polypeptone, 0.2% yeast extract, and 0.1% $MgSO_4$ for 4 days at 30°C. A single colony from the plate was inoculated into a test tube (⌀18 × 180 mm) containing a PET film immersed in YSV medium: 0.01% yeast extract, 0.02% sodium hydrogen carbonate, 0.1% ammonium sulfate, 0.01% calcium carbonate, 0.1% vitamin mixture (0.25% thiamine-HCl, 0.005% biotin, and 0.05% vitamin B12), and 1% of the trace elements in 10 mM phosphate buffer (pH 7.0) and shaken at 300 strokes/min at 30 °C. When the cultivation period was longer than 1 week, the culture fluid was replaced with fresh YSV medium weekly.

Scanning electron microscopy (SEM). After cultivation of *I. sakaiensis* with PET film, the film was immediately soaked in phosphate buffered 2% glutaraldehyde for cell fixation. Post-fixation was performed in 2% osmium tetra-oxide in an ice bath for 3 h. The specimens were dehydrated in 50–100% graded ethanol for 15 min each and critical-point-dried with CO_2. Dried specimens were coated using osmium (Os) plasma ion coater (OPC-80; Nippon Laser & Electronics Lab., Nagoya, Japan) and were examined on a JSM-6320F FE-SEM instrument (JEOL, Tokyo, Japan) at 5 kV. The PET films treated with PETase were washed with 1% SDS, distilled water, and then ethanol. The film was air-dried, coated with Os, and subjected to FE-SEM observation with a JSM-6320F or a FEI Sirion (FEI, Tokyo, Japan) operating at an electron beam intensity of 5 kV.

Reverse-phase high performance liquid chromatography (HPLC) analysis. HPLC was performed on an LC-2010A HT system (Shimadzu) equipped with a Cosmosil $5C_{18}$-AR-II guard column (4.6 × 10 mm) and a Cosmosil $5C_{18}$-AR-II analytical column (4.6 × 250 mm) from Nacalai Tesque (Kyoto, Japan). The mobile phase was methanol/20 mM phosphate buffer (pH 2.5) at a flow rate of 1.0 mL/min, and the effluent was monitored at a wavelength of 240 nm. The typical elution condition was as follows: 0 to 15 min, 25% (v/v) methanol; 15 to 25 min, 25–100% methanol linear gradient.

Ethyl acetate extraction. Culture fluid (5 mL) of *I. sakaiensis* grown on PET film was centrifuged (5,000 × *g*, 10 min, 4°C) to remove the cells. The supernatant was adjusted to pH 2.0 using 2M HCl and extracted with 10 mL of ethyl acetate. The ethyl acetate layer was recovered and evaporated. The residue was dissolved in 250 μL of 16 mM phosphate buffer (pH 2.5)

including 20 % (v/v) DMSO, centrifuged (22,140 × *g*, 15 min, 25°C), and filtered through Cosmo Nice Filter-S with 0.45 μm pore size (Nacalai Tesque).

Whole genome analysis. *I. sakaiensis* cells were cultivated in NBRC 802 medium with shaking for 3 days. Genomic DNA was extracted using the Wizard Genomic DNA purification kit (Promega, Madison, WI) and purified by phenol:chloroform:isoamyl alcohol (25:24:1, v/v/v) extraction. The purified gDNA was fragmented with an Acoustic Solubilizer (Covaris, Woburn, MA) and converted to libraries for next-generation sequencing with Illumina kits (San Diego, CA). Libraries were prepared with the Paired-End Sample Preparation Kit to produce the PE library and the TruSeq DNA PCR-Free Sample Prep Kit to produce the PF library. Sequencing of 80 bp for the PE library and 119 bp for the PF library was performed using the Genome Analyzer IIx (Illumina). The reads were assembled into contigs, with a size of at least 200 bp using CLC Genomics Workbench version 6.5.1 (CLC Bio, Cambridge, MA). The contig sequences were uploaded onto the Rapid Annotation using Subsystem Technology (RAST) server (*20*) for gene annotation.

RNA-Seq analysis. *I. sakaiensis* strain was grown on a 1.5% agarose NBRC 802 medium for 4 days at 30°C. A single colony from the plate was inoculated into fresh liquid NBRC 802 medium and shaken for 3 days at 30°C. The cells were harvested by centrifugation (5,000 × *g*, 5 min, 4°C), washed, and resuspended in the YSV medium. The resuspended cells were inoculated into a test tube (⌀24 × 200 mm) containing 15 mL of YSV medium with PET film (2 cm × 2.5 cm), or 0.075% (w/v) of either maltose monohydrate (maltose) (Nacalai Tesque), disodium terephthalate (TPA-Na) (Tokyo Chemical Industry, Tokyo, Japan), or bis(hydroxyethyl)

terephthalate (BHET) (Sigma-Aldrich, St. Louis, MO) as the major carbon/energy source. At the mid-log phase, 2 mL of culture was harvested and immediately combined with 4 mL of RNAprotect Bacteria Reagent (Qiagen, Valencia, CA). The RNA was extracted and purified using an RNeasy Mini kit (Qiagen) with optional on-column gDNA cleavage. The quality of the RNA was assessed by using a Bioanalyzer 2100 with an RNA 6000 Pico kit from Agilent Technologies (Santa Clara, CA). Bacterial 16S and 23S ribosomal RNAs were subtracted from total RNA with the Ribo-Zero Magnetic kit for gram-negative bacteria (Epicentre, Madison, WI). The enriched mRNA fraction was converted to an RNA-Seq library using ScriptSeq v2 RNA-Seq Library Preparation Kit (Epicentre) with multiplexing adaptors. Each library was hybridized onto a flow cell and sequenced with a Genome Analyzer IIx according to the manufacturer's instructions (Illumina). The draft genome sequence of *Ideonella sakaiensis* was uploaded onto the CLC Genomics Workbench software version 6.5.1 and used as a reference. Reads were mapped on the genome if the fraction of the read that aligned with the reference genome was greater than 0.9 and if the read matched other regions of the reference genome at less than 10 nucleotide positions. The RNA-Seq gene expression patterns were clustered using the K-means clustering method with Euclidean distance on the CLC Genomics Workbench software version 6.5.1. The RNA-Seq output data were analyzed for statistical significance by using the proportion-based test of Baggerly et al. (*21*).

Protein preparation. The genes for PETase (GenBank accession number, GAP38911.1), MHETase (GenBank accession number, GAP38373.1), TfH (GenBank accession number, WP_011291330), LCC (GenBank accession number, AEV21261), and FsC (PDB accession number, 1CEX_A) were commercially synthesized with codon optimization for expression in

156 *Escherichia coli* cells (Operon Biotechnology, Tokyo, Japan). The nucleotide sequence
157 corresponding to the signal peptide was predicted using the LipoP 1.0 server
158 (http://www.cbs.dtu.dk/services/LipoP) (*22*) and removed from the synthetic DNA. The genes
159 for PETase, TfH, and LCC were individually cloned into the NdeI (5′ end) and XhoI (3′ end)
160 sites of pET-21b vector (Novagen, San Diego, CA) through fusion to its C-terminal hexa-
161 histidine tag-coding sequence. Genes were expressed in *E. coli* BL21 (DE3) CodonPlus RIPL
162 competent cells (Agilent Technologies) by 0.1 mM IPTG induction at 16°C. The genes for
163 MHETase and FsC were individually cloned into the NdeI (5′ end) and XbaI (3′ end) sites of
164 pCold II vector (Takara Bio, Otsu, Japan) through fusion to the N-terminal hexa-histidine tag
165 sequence. Genes were expressed in *E. coli* Rosetta-gami B(DE3) (Merck Millipore, Darmstadt,
166 Germany) by 0.1 mM IPTG induction at 15°C. The *E. coli* cells were harvested by centrifugation
167 (5,000 × *g*, 5 min, 4°C) and resuspended in lysis buffer (50 mM Tris-HCl, pH 7.5, 300 mM NaCl,
168 20 mM imidazole). Cells were disrupted by sonication on ice and the lysate was clarified by
169 centrifugation (15,000 × *g*, 20 min, 4°C). The supernatant was applied to the His-Accept nickel
170 column (Nacalai Tesque). After washing unbound proteins with the lysis buffer, the bound
171 proteins were eluted with elution buffer (50 mM Tris-HCl, pH 7.5, 300 mM NaCl, 250 mM
172 imidazole), and the buffer was exchanged for 50 mM Na_2HPO_4-HCl, pH 7.0, and 100 mM NaCl
173 on a PD-10 gel filtration column (GE Healthcare, Piscataway, NJ). The purified protein
174 concentration was determined based on the calculated molar extinction coefficient at 280 nm.
175
176 **Enzyme assays for PET film.** Purified protein was incubated with PET film (⌀6 mm), in 300 μL
177 of buffer containing 50 mM Na_2HPO_4-HCl (pH 6.0–8.0), Bicine-NaOH (pH 8.0–9.0), or 50 mM
178 glycine-NaOH (pH 9.0–10). The reaction was terminated by dilution of the aqueous solution

with 18 mM phosphate buffer (pH 2.5) containing 10 % (v/v) DMSO followed by heat treatment (85°C, 10 min). The supernatant obtained by centrifugation (15,000 × *g*, 10 min) was analyzed by HPLC. After the reaction, the PET film was washed with 1% SDS, distilled water, and ethanol. Then, the film was air-dried for SEM observation.

Enzyme assays for highly crystallized PET (hcPET). Purified protein was incubated with hcPET cut out from commercial PET bottle (⌀6 mm), in 300 μL of buffer containing 50 mM Bicine-NaOH (pH 9.0) for 18 h at 30°C. The reaction was stopped by dilution of the aqueous solution with 160 mM phosphate buffer (pH 2.5) including 20 % (v/v) DMSO, followed by heat treatment (85°C, 10 min). The supernatant obtained by centrifugation (15,000 × *g*, 10 min) was then analyzed by HPLC.

Enzyme assays for bis(2-hydroxyethyl)terephthalic acid (BHET). The protein was incubated with 0.9 mM BHET at 30°C in 40 mM Na_2HPO_4-HCl (pH 7.0), 80 mM NaCl, and 20 % (v/v) DMSO. The reaction was stopped by dilution with 16 mM phosphate buffer (pH 2.5) including 20 % (v/v) DMSO, followed by heat treatment (80°C, 10 min). The supernatant obtained by centrifugation (15,000 × *g*, 10 min) was then analyzed by HPLC.

Enzymatic preparation of mono(2-hydroxyethyl)terephthalic acid (MHET). Four mM BHET was incubated with 50 nM PETase in 40 mM Na_2HPO_4-HCl (pH 7.0), 80 mM NaCl, and 20 % (v/v) DMSO at 30°C. After complete hydrolysis of BHET to MHET was confirmed by HPLC, the protein was removed from the reaction mixture with Amicon Ultra 10 kDa (Merck Millipore), resulting in a 4 mM MHET solution.

Kinetic analysis of MHETase. Two nM MHETase protein was incubated with 1 μM to 25 μM of MHET in 40 mM Na_2HPO_4-HCl (pH 7.0), 80 mM NaCl, and 20 % (v/v) DMSO at 30°C. The reaction was stopped by adding an equal amount of 160 mM phosphate buffer (pH 2.5) including 20 % (v/v) DMSO. The TPA produced was detected by HPLC analysis. Initial rates were plotted against MHET concentrations and the kinetic parameters were determined by using the Michaelis–Menten equation utilizing Graph Pad Prism version 6.01 (GraphPad Software, San Diego, CA).

Enzymatic activities of MHETase for the small aromatic esters. MHETase protein (50 nM) was incubated with 1 mM ethyl gallate, ethyl ferulate, or chlorogenic acid hydrate (Tokyo Chemical Industry), in 40 mM Na_2HPO_4-HCl (pH 7.0), 80 mM NaCl, and 20 % (v/v) DMSO at 30°C for 18 h. The reaction mixture was diluted with 16 mM phosphate buffer (pH 2.5) including 20 % (v/v) DMSO, heat treated (80°C, 10 min), and analyzed by HPLC. Gallic acid hydrate (Tokyo Chemical Industry), ferulic acid (LKT Laboratories, St. Paul, MN), and caffeic acid (Tokyo Chemical Industry) were used as standards for identification of hydrolytic products of ethyl gallate, ethyl ferulate, and chlorogenic acid hydrate, respectively.

Enzyme activities for *p*NP-aliphatic esters. Enzyme was incubated with 1 mM *para*-nitrophenol (*p*NP)-acetate, *p*NP-butyrate, *p*NP-octanoate (Sigma-Aldrich), or *p*NP-hexanoate (Tokyo Chemical Industry) in 45 mM Na_2HPO_4-HCl (pH 7.0), 90 mM NaCl, and 10% (v/v) DMSO at 30°C. The production of *p*NP was continuously monitored at a wavelength of 415 nm. The specific activity was calculated from the initial catalytic rate with linearity.

Phylogenetic analysis. Multiple amino acid sequences were aligned with ClustalW (http://www.ebi.ac.uk/clustalw) and the guide tree was obtained based on the neighbor-joining method using p-distance model in DNA Data bank of Japan (DDBJ; http://clustalw.ddbj.nig.ac.jp/top-e.html). The TreeView software (http://taxonomy.zoology.gla.ac.uk/rod/treeview.html) was utilized to visualize the tree.

Transcription start site (TSS) identification for ISF6_4831 and ISF6_0224 genes. The RNA-Seq library was mapped on the target gene-sitting DNA strand by using the CLC Genomics Workbench software version 6.5.1. The coverage data was scanned by moving through the gene of interest and the upstream intergenic region toward 5′ direction. The averaged coverage score of the biological replicates at a single nucleotide position was compared with that at the last position. In this analysis, the nucleotide position that displayed the largest drop-off value was identified as TSS.

Protein homolog search on the fully sequenced genomes. The Mirrortree server (http://csbg.cnb.csic.es/mtserver/index.php) (*23*) was utilized. Homologs with ≥30% identity, $\leq 1e^{-5}$ E-value, and ≥60% coverage were BLAST-searched against the Integr8 genome database implemented in this server.

16S rRNA phylogenetic analysis. The 16S rRNA sequences were obtained from the Silva web database (http://www.arb-silva.de/) and aligned with the MEGA6 software (*24*) to construct a maximum likelihood phylogenetic tree.

249

Supplementary Texts:

Text S1.

By directional RNA-Seq analysis of *I. sakaiensis* cells growing on PET film, we searched the transcription start sites (TSSs) of PETase and MHETase to accurately determine their ORFs (Fig. S14). These TSSs were -41 nt and -44 nt from the respective translation start sites that were computationally determined with the RAST program. Therefore, the ORFs were experimentally validated. Next, we utilized the LipoP 1.0 program (*22*) to predict the protein localization in *I. sakaiensis* cells. PETase was predicted to be a secretory protein whose N-terminal 27-amino-acid sequence is cleaved off by type I signal peptidase (LipoP 1.0 score = 18.7613). MHETase was predicted to be a lipoprotein whose N-terminal 17-amino-acid sequence is cleaved off by type II signal peptidase (LipoP 1.0 score = 20.5281). The +2 position relative to the predicted MHETase cleavage site is taken by an alanine that potentially directs the protein to the outer membrane (*22*).

Text S2.

I. sakaiensis harbors a gene cluster that is highly identical with two TPA degradation gene clusters identified in *Comamonas* sp. E6 (Fig. S11 and Table S5). Sasoh et al. demonstrated that both clusters contribute to the conversion of TPA to PCA (*25*). Furthermore, Hosaka et al. identified the TPA-uptake system composed of a novel tripartite aromatic acid transporter composed of TpiA–TpiB membrane protein complex and TPA-binding protein TphC (*17*), whose homologs are all encoded on the *I. sakaiensis* genome (Table S5). *I. sakaiensis* also harbors a set of genes whose product shares identity with the well-studied protocatechuate 3,4-dioxygenase from *Pseudomonas putida* (*26, 27*), accounting for 52% (E-value = $1e^{-66}$) for the α-

subunit (GenBank accession number, 3PCG:C) and 60% (E-value = $2e^{-101}$) for the β-subunit (GenBank accession number, 3PCG:N).

Supplementary Tables:

Table S1. Results for sequencing, assembly, and ORF determination of the *I. sakaiensis* 201-F6 genome

Total reads (average length)	PE library	51,405,387 (80.0 nt)
	PF library	26,786,010 (119 nt)
Reads after trimming (average length)	PE library	51,345,961 (74.9 nt)
	PF library	26,758,947 (98.1 nt)
Mapped reads (%)		99.6
Contigs		227
Shortest contig size (bp)		207
Longest contig size (bp)		290,390
Total contig size (bp)		6,142,063
Average coverage		1,050
N25 (bp)		177,646
N50 (bp)		96,108
N75 (bp)		57,621
GC content (%)		72.9
CDSs		5,527
RNAs		47

Table S2. Activities of PET hydrolytic enzymes with known polypeptide sequence.

Enzyme		**PETase**	**TfH**	**LCC**	**FsC**	**Thc_Cut1**	**Thc_Cut2**	**Thf42_Cut1**	**Tha_Cut1**	**Thh_Est**	**Cut190 S226P/R228S**	**HiC**	**BsEstB**
Accession number		GAP38373.1	WP_011291330.1	AEV21261.1	1CEX	ADV92526.1	ADV92527.1	ADV92528.1	ADV92525.1	AFA45122.1	BAO42836.1 (wild-type)	4OYY	ADH43200.1
Identity with PETase (E-value)		-	51% ($1e^{-87}$)	49% ($2e^{-79}$)	45% (0.15)	52% ($1e^{-87}$)	50% ($4e^{-85}$)	51% ($1e^{-77}$)	53% ($3e^{-85}$)	49% ($1e^{-83}$)	45% ($2e^{-71}$)	67% (2.7)	23% (0.52)
Organism		*Ideonella sakaiensis* 201-F6	*Thermobifida fusca* DSM43793	Uncultured bacterium	*Fusarium solani* pisi	*Thermobifida cellulosilytica* DSM44535	*Thermobifida cellulosilytica* DSM44535	*Thermobifida fusca* DSM44342	*Thermobifida alba* DSM43185	*Thermobifida halotolerans* DSM44931	*Saccharomonospora viridis* AHK190	*Humicola insolens*	*Bacillus subtilis* 4P3-11
Hydrolytic activity	PET (Temp.[a])	Yes (20–45°C)	Yes (55°C)	Yes (50°C)	Yes (30–55°C)	Yes (50°C)	Yes (50°C)	Yes (50°C)	Yes (50°C)	Yes (50°C)	Yes (60, 65°C)	Yes (30–85°C)	Yes (-)
	3PET[b]	-	Yes	-	Yes	Yes	Yes	Yes	Yes	Yes	-	Yes	Yes
	BHET	Yes	Yes	-	Yes	-	-	-	-	-	-	Yes	Yes
	MHET	No	Yes	-	Yes	Yes	Yes	Yes	No	-	-	-	Yes
	*p*NP-aliphatic esters (carbons[c])	Yes (2, 4, 6, 8)	Yes (4)	Yes (2, 4, 6, 8, 12, 14, 16, 18)	Yes (4, 14)	Yes (2, 4)	Yes (2, 4)	Yes (2, 4)	Yes (2, 4)	Yes (2, 4)	Yes (2, 4, 6, 8, 10)	Yes (2, 4)	Yes (2, 4)
References		This study	(*10, 28, 29*)	(*11*)	(*12, 29-31*)	(*32*)	(*32*)	(*32*)	(*8*)	(*33*)	(*34*)	(*8, 31*)	(*35*)

[a]Reported temperature range in which the activity was detected.
[b]Bis(benzoyloxyethyl) terephthalate
[c]The number of the carbons in the aliphatic chain of *p*NP-aliphatic esters that were hydrolyzed by the enzyme.

Table S3. Results of RNA-Seq read mapping onto the *I. sakaiensis* draft genome

Carbon source	Biological replicate #	Total reads (average length)	Reads after trimming (average length)	Uniquely mapped reads (ratio of mapped reads)
Maltose	1	9,369,188 (119 nt)	6,217,946 (91.2 nt)	3,656,339 (58.8%)
	2	8,529,397 (119 nt)	5,487,432 (90.1 nt)	3,016,647 (55.0%)
Disodium terephthalate (TPA-Na)	1	8,468,195 (119 nt)	5,413,150 (85.0 nt)	2,719,573 (50.2%)
	2	10,350,890 (119 nt)	6,294,206 (60.5 nt)	2,160,743 (34.3%)
Bis(hydroxyethyl) terephthalate (BHET)	1	7,355,445 (119 nt)	4,540,613 (79.1 nt)	2,148,068 (47.3%)
	2	8,632,578 (119 nt)	5,352,601 (69.3 nt))	2,204,815 (41.2%)
PET film	1	9,304,847 (119 nt)	6,871,354 (91.2 nt)	3,541,450 (51.5%)
	2	11,817,517 (119 nt)	8,117,398 (82.0 nt)	3,697,272 (45.5%)

Table S4. Twenty most highly expressed protein-coding genes in *I. sakaiensis* grown on PET film[a]

		Averaged RPKM[c]			
ORF[b] #	Function[b]	Maltose	TPA-Na	PET	BHET
ISF6_4831	lipase	3207	1610	49050	1207
ISF6_0224	chlorogenate esterase	124	7828	46452	2828
ISF6_0364	uncharacterized protein ImpD	20301	17063	31504	7294
ISF6_0227	ortho-halobenzoate 1,2-dioxygenase alpha-ISP protein OhbB	56	29170	26050	14098
ISF6_1126	hypothetical protein	19169	21319	21049	22173
ISF6_4707	putative exported protein	1089	9422	19013	9212
ISF6_0529	aldehyde dehydrogenase	36	37	15929	30
ISF6_0228	ortho-halobenzoate 1,2-dioxygenase beta-ISP protein OhbA	38	18609	15813	9075
ISF6_4223	bacterioferritin	29764	35250	14515	11515
ISF6_0226	putative exported protein	36	14963	12999	7547
ISF6_0271	outer membrane porin protein BP0840 precursor	10800	7940	8990	12517
ISF6_4411	flagellin protein FlaA	5766	8758	8833	808
ISF6_0363	uncharacterized protein ImpC	6520	6787	8811	2502
ISF6_5356	DNA topoisomerase III	9523	8371	8092	8271
ISF6_1290	ribosome hibernation protein YhbH	880	4765	6502	362
ISF6_2225	SSU ribosomal protein S13p (S18e)	18608	5422	6128	24812
ISF6_1504	outer membrane protein (porin)	11585	12384	6048	15639
ISF6_0559	hypothetical protein	79	5146	5646	3262
ISF6_0064	outer membrane protein A precursor	7427	7635	5536	8765
ISF6_4296	chemotaxis regulator	3302	4035	5419	752

[a]*I. sakaiensis* was grown in YSV medium containing maltose, TPA-Na, PET film, or BHET, and the mRNAs from exponentially growing cells were subjected to RNA-Seq analysis.

[b]Open reading frames (ORFs) and their protein functions were annotated using the RAST server.

[c]The RPKM (reads per kilobase of exon model per million mapped reads) values were determined by CLC Genomics Workbench v. 6.5.1 based on the Illumina reads. Values are calculated from two biological replicates (Supplementary Table 3).

289 **Table S5. Putative 201-F6 proteins involved in TPA degradation and their characterized homologs in *Comamonas* sp. E6**

290

ORF#	Homolog(s) in *Comamonas* sp. E6[a]			
	Gene	Identity (E-value)[b]	Function	Reference
ISF6_0225	*tphR*$_{I}$	72% (3e^{-36})	IclR-type transcriptional regulator	(*25*)
	tphR$_{II}$	72% (3e^{-36})		
ISF6_0226	*tphC*$_{I}$	64% (1e^{-156})	periplasmic TPA binding receptor	(*17, 25*)
	tphC$_{II}$	64% (1e^{-156})		
ISF6_0227	*tphA2*$_{I}$	79% (0)	large subunit of the oxygenase component of TPA 1,2-dioxygenase (TPADO)	(*25*)
	tphA2$_{II}$,	79% (0)		
ISF6_0228	*tphA3*$_{I}$	67% (5e^{-79})	small subunit of the oxygenase component of TPADO	(*25*)
	tphA3$_{II}$	67% (1e^{-77})		
ISF6_0229	*tphB*$_{I}$	67% (2e^{-140})	1,2-dihydroxy-3,5-cyclohexadiene-1,4-dicarboxylate (DCD) dehydrogenase	(*25*)
	tphB$_{II}$	67% (7e^{-140})		
ISF6_0230	*tphA1*$_{I}$	59% (1e^{-144})	reductase component of TPADO	(*25*)
	tphA1$_{II}$	59% (3e^{-145})		
ISF6_0076	*tpiB*	46% (2e^{-44})	small transmembrane protein of the aromatic acids transporter	(*17*)
ISF6_0077	*tpiA*	78% (0)	large transmembrane protein of the aromatic acids transporter	(*17*)

[a]*Comamonas* sp. E6 harbors two almost identical TPA degradation gene clusters, *tphR*$_{I}$*C*$_{I}$*A2*$_{I}$*A3*$_{I}$*B*$_{I}$*A1*$_{I}$ and *tphR*$_{II}$*C*$_{II}$*A2*$_{II}$*A3*$_{II}$*B*$_{II}$*A1*$_{II}$ (*25*).
[b]Identity with the corresponding 201-F6 protein was determined by their alignment using BLASTp program.

291

292

293

Supplementary Figures:

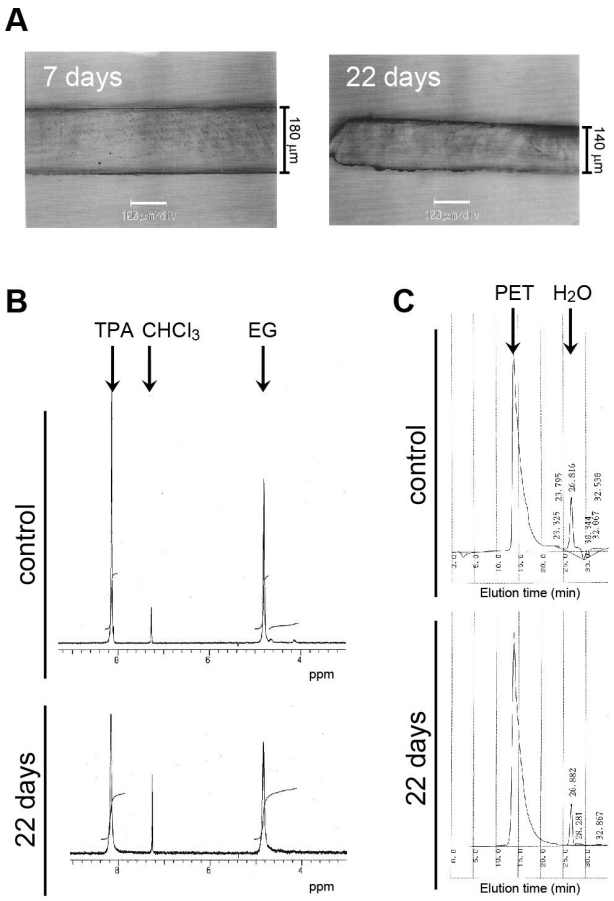

Fig. S1. Analyses of PET films degraded by the consortium No. 46.
No. 46 was cultured with PET film (20 × 15 × 0.2 mm) in MLE medium at 30°C. The medium was changed every 2 weeks. The degraded PET films were washed, dried, and analyzed. (**A**) Microscopic observation of cross-sections of the PET film cultivated for 7 days and 22 days. Horizontal bars indicate 100 μm. (**B**) ^{1}H-NMR spectra of intact PET film (control) and PET film after 22 days of bacterial cultivation (22 days). The integral values of peaks of terephthalic acid (TPA) and ethylene glycol (EG) were almost identical in both samples, indicating that the degradation proceeded only at the film surface. (**C**) GPC profiles of intact PET film (control) and PET film after 22 days of bacterial cultivation (22 days). The elution profiles for PET were almost identical in both samples, indicating that the degradation proceeded only at the PET film surface.

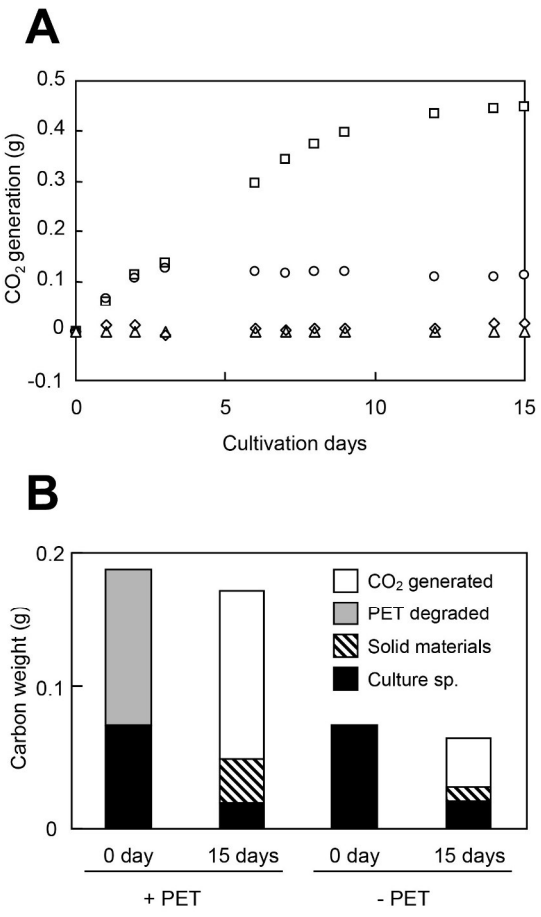

Fig. S2. CO_2 generation during growth of No. 46 on PET film.
(**A**) Time course of CO_2 generation from various cultures. No. 46 was cultivated in 270 mL of MLE medium containing PET films (14×150×0.2 mm, 4 sheets) at 28°C. Results are shown for culture in the presence of No. 46 and PET (squares), No. 46 in the absence of PET (circles), PET in the absence of No. 46 (diamonds), and the pure medium (triangles). Three analyses were performed in the presence of PET and two in the absence thereof, with the respective data averaged. (**B**) Conversion of degraded PET to CO_2. After 15 days of cultivation, the carbon weight of generated CO_2, degraded PET, biofilm-like (solid) materials, and culture supernatant was measured, and compared with those before cultivation.

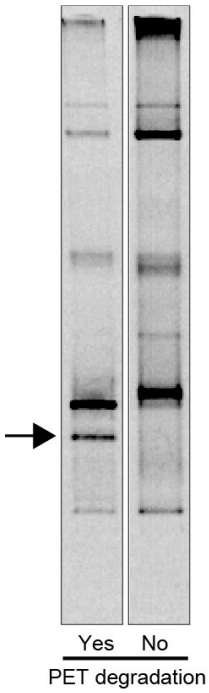

Fig. S3. DGGE analysis of microbial consortia derived from No. 46.
DGGE profiles of the V3–V5 region of 16S rDNA of microbial consortia derived from No. 46 (left, a consortium with PET degradation activity; right, a consortium without PET degradation activity) were compared. The arrow indicates the band corresponding to *I. sakaiensis* 201-F6.

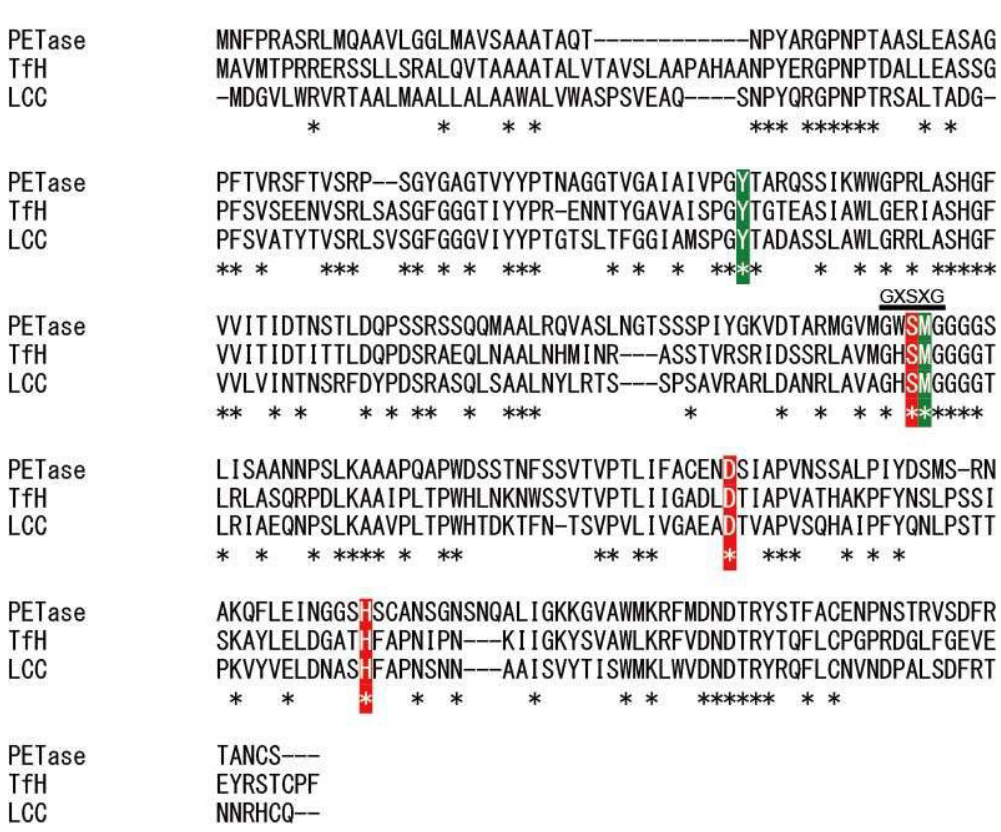

Fig. S4. Amino acid sequence alignment of PETase, TfH, and LCC. Based on the study of TfH (*36*), the amino acid residues forming a catalytic triad (shaded in red) and an oxyanion hole (shaded in green) were identified. The GXSXG motif conserved in α/β-fold hydrolases such as esterases and lipases is overlined. *, conserved residue.

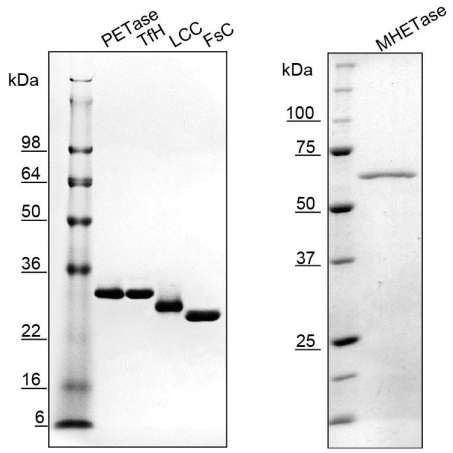

Fig. S5. Purification of the hexa-histidine-tagged enzymes studied.
PETase (28.6 kDa, 1 μg), TfH (29.2 kDa, 1 μg), LCC (28.8 kDa, 1 μg), FsC (23.7 kDa, 1 μg), and MHETase (62.8 kDa, 0.5 μg) were loaded on a 12.5% SDS-PAGE gel, and stained with Coomassie Brilliant Blue G-250.

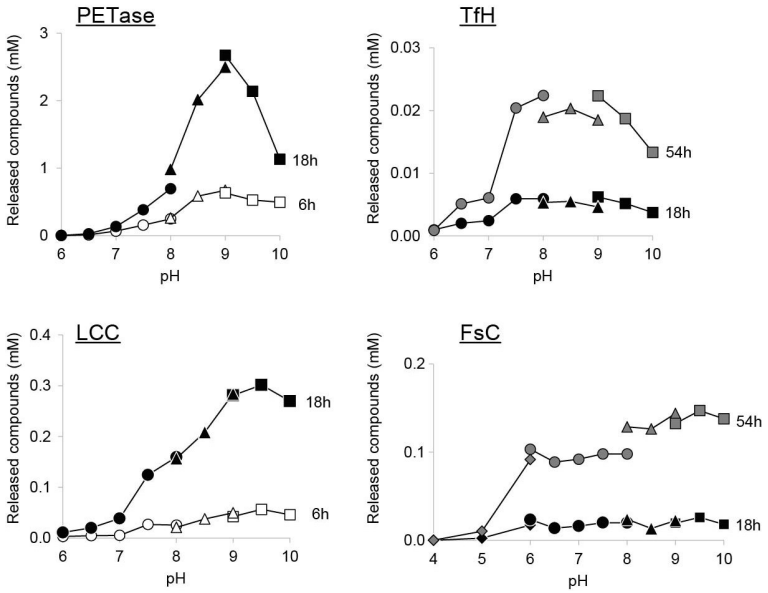

Fig. S6. Effect of pH on enzymatic PET film hydrolysis.
PETase, TfH, LCC, or FsC was incubated with PET film (⌀6 mm) at 30°C in 50 mM Na_2HPO_4-HCl (circles; pH 6.0–8.0), Bicine-NaOH (triangles; pH 8.0–9.0), and 50 mM glycine-NaOH (squares; pH 9.0–10). The incubation time was 6 and 18 h for PETase and LCC, or 18 and 54 h for TfH and FsC. The enzyme concentration was 50 nM for PETase and 200 nM for TfH, LCC, and FsC. The sum of the detected released compounds (TPA, MHET, and BHET) is shown.

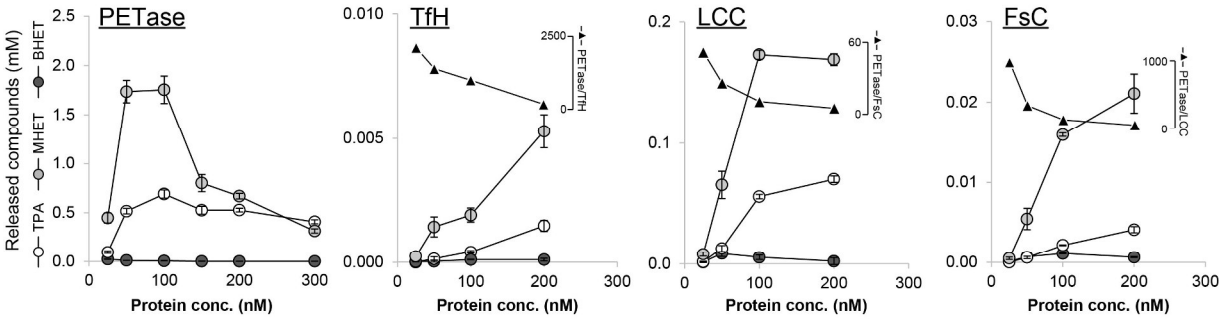

Fig. S7. Effect of enzyme concentration on PET film hydrolysis. PETase, TfH, LCC, or FsC was incubated with PET film (⌀6 mm) in pH 9.0 buffer at 30°C for 18 h. The released products in each supernatant are shown (circles). Markers are shown with standard errors (n≥3). At each protein concentration, the sum of the released compounds (TPA, MHET, and BHET) was compared between PETase and TfH, LCC, or FsC (triangles).

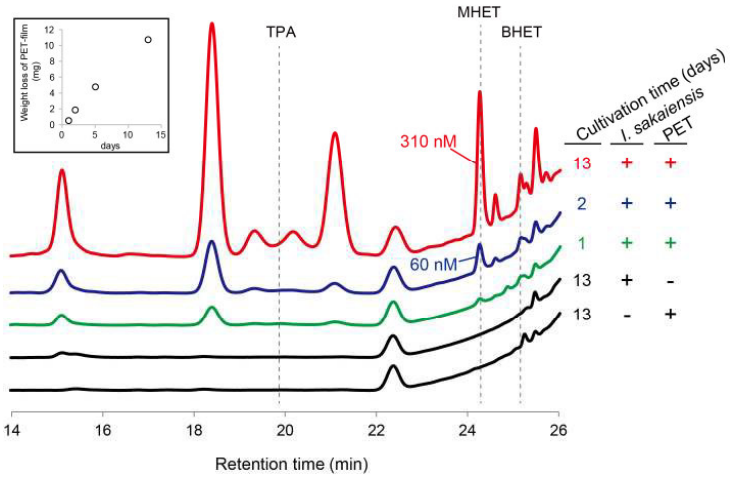

Fig. S8. HPLC spectra of culture supernatants from *I. sakaiensis* grown on PET film.
I. sakaiensis was cultured with or without PET film (20 × 15 × 0.2 mm) for 1, 2, and 13 days, in 5 mL of YSV medium. In addition, PET film alone was incubated in the same culture medium for 13 days. The inset is the time course of PET film degradation by *I. sakaiensis*. The culture supernatant was acidified and extracted with ethyl acetate. The extract was analyzed by reverse-phase HPLC. The retention times of the standards (TPA, MHET, and BHET) are indicated by dashed lines. The weight loss of PET film after 13-day culture was 10.7 mg, which corresponds to 10.2 mM of MHET or TPA units in the 5 mL medium. The MHET concentration in the supernatant after 13-day culture was calculated to be 310 nM, accounting for only 0.003% of MHET units of the degraded PET.

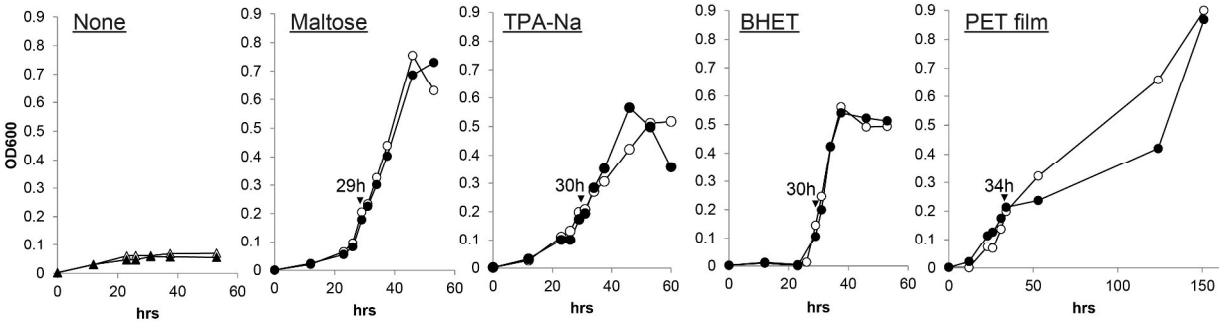

Fig. S9. Growth curves for *Ideonella sakaiensis* grown on either maltose, disodium terephthalate (TPA-Na), bis(hydroxyethyl) terephthalate (BHET), or PET film.
I. sakaiensis was cultured in 15 mL of YSV medium without an additional carbon source (control) or with maltose (0.075%, w/v), TPA-Na (0.075%, w/v), BHET (0.075%, w/v), or PET film (1.4 cm × 2.0 cm), and the optical density at 660 nm of the fluid was monitored. Two independent cultures (#1 biological replicate, open circles; #2 biological replicate, closed circles) were performed for each carbon source. Arrow heads indicate the time at which the cells were harvested for RNA-Seq experiments (Table S3).

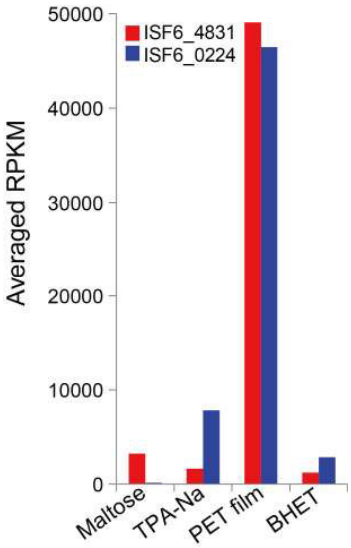

Fig. S10. RNA-Seq transcript levels of ISF6_4831 and ISF6_0224 on four different carbon sources.

I. sakaiensis was grown in YSV medium containing maltose, TPA-Na, PET film, or BHET (Fig. S9), and the mRNAs from exponentially growing cells were subjected to RNA-Seq analysis. The RPKM (reads per kilobase of exon model per million mapped reads) values were determined based on the Illumina reads using the CLC Genomics Workbench v. 6.5.1. The average values from two independent experiments (Table S4) are shown.

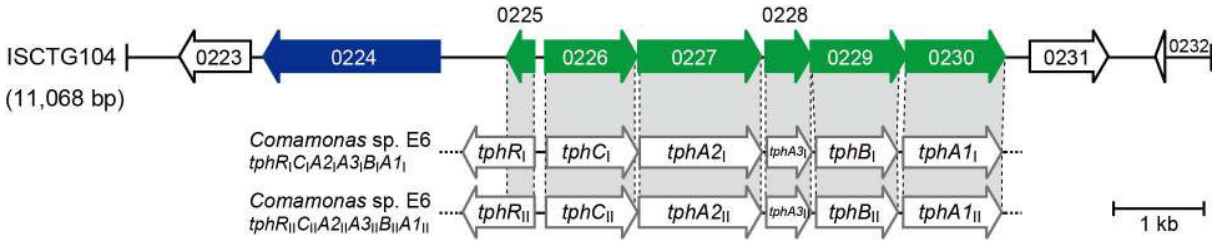

Fig. S11. Schematic illustration of annotated genes on the contig ISCTG104 of the *I. sakaiensis* draft genome. ISF6_0225–0230 were functionally annotated based on the similarity with genes in the two almost identical TPA degradation gene clusters of *Comamonas* sp. strain E6, *tphR*$_{I}$*C*$_{I}$*A2*$_{I}$*A3*$_{I}$*B*$_{I}$*A1*$_{I}$ (GenBank accession, AB238678) and *tphR*$_{II}$*C*$_{II}$*A2*$_{II}$*A3*$_{II}$*B*$_{II}$*A1*$_{II}$ (GenBank accession, AB238679) (*25*): ISF6_0225, IclR-type transcriptional regulator; ISF6_0226, periplasmic TPA binding receptor; ISF6_0227, large subunit of the oxygenase component of TPA 1,2-dioxygenase (TPADO); ISF6_0228, small subunit of the oxygenase component of TPADO; ISF6_0229, 1,2-dihydroxy-3,5-cyclohexadiene-1,4-dicarboxylate (DCD) dehydrogenase; ISF6_0230, TPADO reductase component. The corresponding genes are connected by dashed lines, and the amino acid identity between the gene products is shown in Table S5.

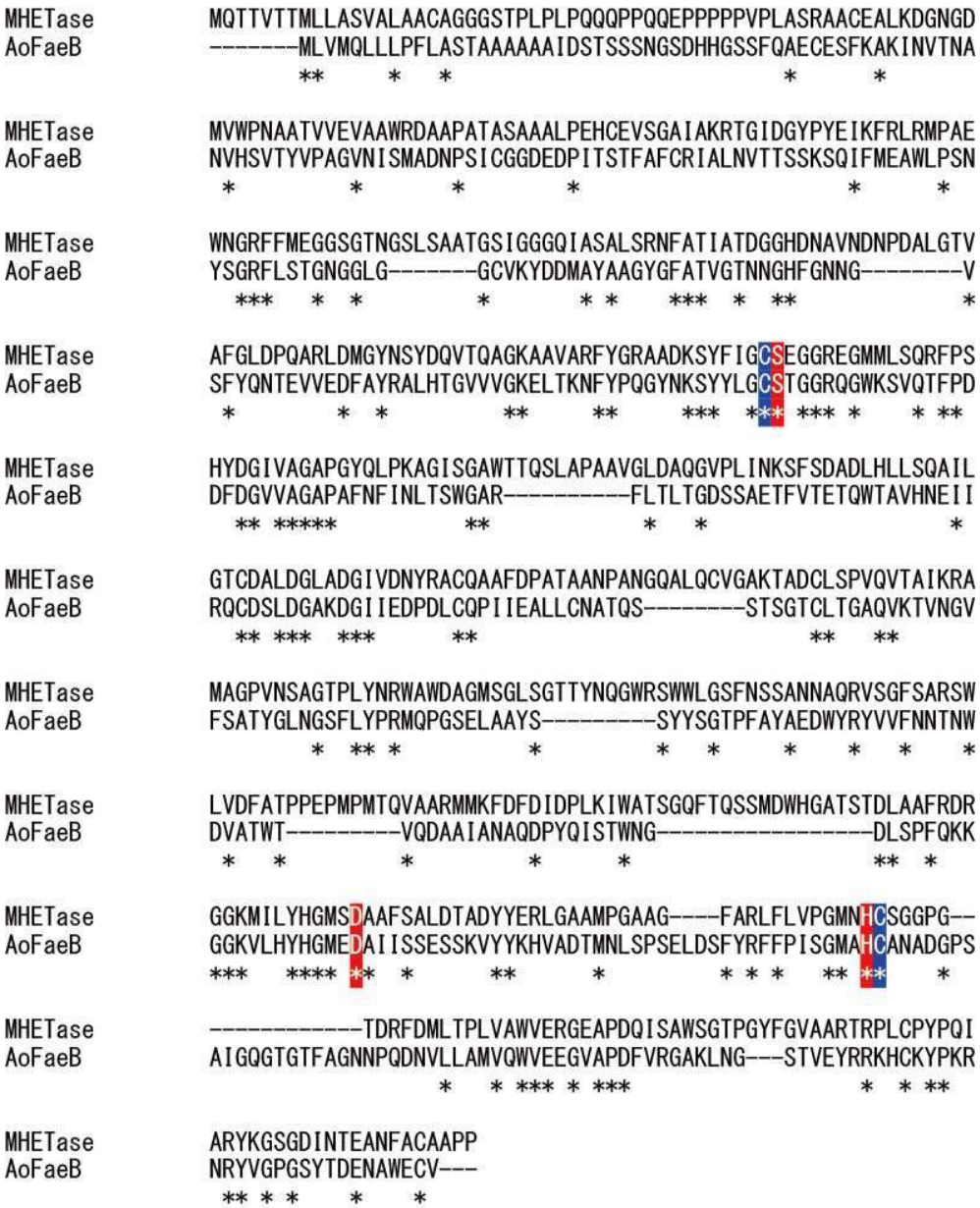

Fig. S12. Amino acid sequence aligment of MHETase (ISF6_0224 protein) and AoFaeB. AoFaeB is a well-characterized feruloyl esterase from *Aspergillus oryzae* strain RIB40 that belongs to the tannase family (*37*). The amino acid residues forming a catalytic triad are shaded in red. Disulfide bond forming cysteines that connect the catalytic serine and histidine are shaded in blue. They are completely conserved among biochemically characterized tannase family proteins (*15*). *, conserved residue.

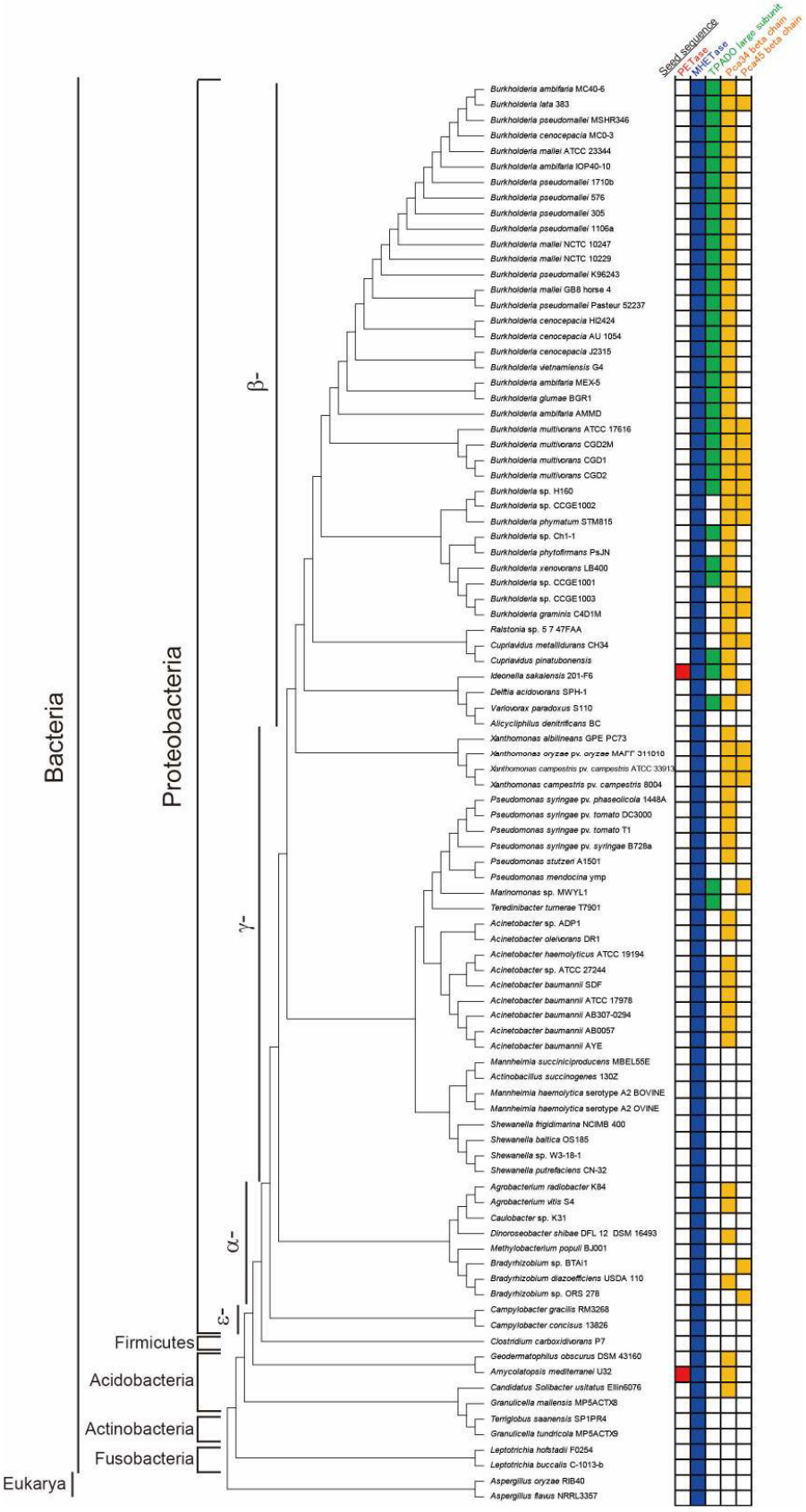
Seed sequence
PETase
MHETase
TPADO large subunit
Pca34 beta chain
Pca45 beta chain
Bacteria
Proteobacteria
β-
γ-
α-
ε-
Firmicutes
Acidobacteria
Actinobacteria
Fusobacteria
Eukarya
Burkholderia ambifaria MC40-6
Burkholderia lata 383
Burkholderia pseudomallei MSHR346
Burkholderia cenocepacia MC0-3
Burkholderia mallei ATCC 23344
Burkholderia ambifaria IOP40-10
Burkholderia pseudomallei 1710b
Burkholderia pseudomallei 576
Burkholderia pseudomallei 305
Burkholderia pseudomallei 1106a
Burkholderia mallei NCTC 10247
Burkholderia mallei NCTC 10229
Burkholderia pseudomallei K96243
Burkholderia mallei GB8 horse 4
Burkholderia pseudomallei Pasteur 52237
Burkholderia cenocepacia HI2424
Burkholderia cenocepacia AU 1054
Burkholderia cenocepacia J2315
Burkholderia vietnamiensis G4
Burkholderia ambifaria MEX-5
Burkholderia glumae BGR1
Burkholderia ambifaria AMMD
Burkholderia multivorans ATCC 17616
Burkholderia multivorans CGD2M
Burkholderia multivorans CGD1
Burkholderia multivorans CGD2
Burkholderia sp. H160
Burkholderia sp. CCGE1002
Burkholderia phymatum STM815
Burkholderia sp. Ch1-1
Burkholderia phytofirmans PsJN
Burkholderia xenovorans LB400
Burkholderia sp. CCGE1001
Burkholderia sp. CCGE1003
Burkholderia graminis C4D1M
Ralstonia sp. 5 7 47FAA
Cupriavidus metallidurans CH34
Cupriavidus pinatubonensis
Ideonella sakaiensis 201-F6
Delftia acidovorans SPH-1
Variovorax paradoxus S110
Alicycliphilus denitrificans BC
Xanthomonas albilineans GPE PC73
Xanthomonas oryzae pv. oryzae MAFF 311010
Xanthomonas campestris pv. campestris ATCC 33913
Xanthomonas campestris pv. campestris 8004
Pseudomonas syringae pv. phaseolicola 1448A
Pseudomonas syringae pv. tomato DC3000
Pseudomonas syringae pv. tomato T1
Pseudomonas syringae pv. syringae B728a
Pseudomonas stutzeri A1501
Pseudomonas mendocina ymp
Marinomonas sp. MWYL1
Teredinibacter turnerae T7901
Acinetobacter sp. ADP1
Acinetobacter oleivorans DR1
Acinetobacter haemolyticus ATCC 19194
Acinetobacter sp. ATCC 27244
Acinetobacter baumannii SDF
Acinetobacter baumannii ATCC 17978
Acinetobacter baumannii AB307-0294
Acinetobacter baumannii AB0057
Acinetobacter baumannii AYE
Mannheimia succiniciproducens MBEL55E
Actinobacillus succinogenes 130Z
Mannheimia haemolytica serotype A2 BOVINE
Mannheimia haemolytica serotype A2 OVINE
Shewanella frigidimarina NCIMB 400
Shewanella baltica OS185
Shewanella sp. W3-18-1
Shewanella putrefaciens CN-32
Agrobacterium radiobacter K84
Agrobacterium vitis S4
Caulobacter sp. K31
Dinoroseobacter shibae DFL 12 DSM 16493
Methylobacterium populi BJ001
Bradyrhizobium sp. BTAi1
Bradyrhizobium diazoefficiens USDA 110
Bradyrhizobium sp. ORS 278
Campylobacter gracilis RM3268
Campylobacter concisus 13826
Clostridium carboxidivorans P7
Geodermatophilus obscurus DSM 43160
Amycolatopsis mediterranei U32
Candidatus Solibacter usitatus Ellin6076
Granulicella mallensis MP5ACTX8
Terriglobus saanensis SP1PR4
Granulicella tundricola MP5ACTX9
Leptotrichia hofstadii F0254
Leptotrichia buccalis C-1013-b
Aspergillus oryzae RIB40
Aspergillus flavus NRRL3357

Fig. S13. Homolog distribution of PETase and TPA catabolic enzymes in MHETase homolog harboring organisms.

The MHETase homologs were searched on the Integr8 fully sequenced genome database implemented on the Mirrortree server. Maximum likelihood phylogenetic tree for the 16S rRNA sequences of the corresponding organisms was constructed (left). Homologs for PETase and TPA catabolic enzymes in these organisms were BLAST-searched. As protein seed sequences, PETase, TPADO (the oxygenase component of TPA 1,2-dioxygenase) large subunit, and protocatechuate 3,4-dioxygenase (Pca34) beta chain, all from *I. sakaiensis*, were utilized. Homologs for protocatechuate 4,5-dioxygenase (Pca45), another PCA ring-cleavage enzyme (*38*), were also searched using Pca45 beta subunit from *Comamonas* sp. strain E6 (accession number, BAI50715) (*39*). Presence of the homolog(s) in the genome is indicated by a colored box (right).

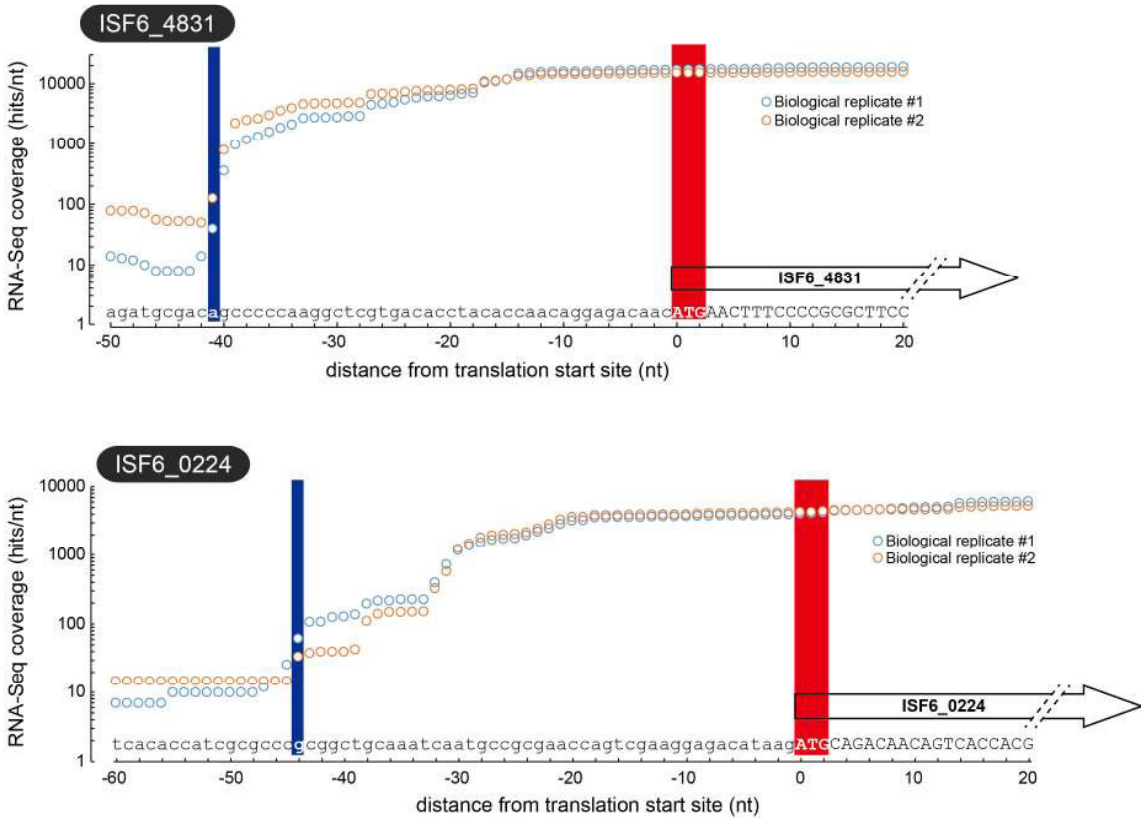

Fig. S14. RNA-Seq coverage-based transcription start site (TSS) identification for ISF6_4831 and ISF6_0224 genes. Directional RNA-Seq reads obtained from *I. sakaiensis* cells grown on PET film (Fig. S9, rightmost panel) were mapped onto the specific DNA strand the target gene is located on. The blue line indicates the TSS determined by RNA-Seq coverage. The red line indicates the start codon predicted by RAST genome analysis.

References and Notes:

1. V. Sinha, M. R. Patel, J. V. Patel, Pet waste management by chemical recycling: A review. *J. Polym. Environ.* **18**, 8–25 (2010). doi:10.1007/s10924-008-0106-7
2. R. J. Müller, I. Kleeberg, W. D. Deckwer, Biodegradation of polyesters containing aromatic constituents. *J. Biotechnol.* **86**, 87–95 (2001). doi:10.1016/S0168-1656(00)00407-7
3. D. Kint, S. Munoz-Guerra, A review on the potential biodegradability of poly(ethylene terephthalate). *Polym. Int.* **48**, 346–352 (1999). doi:10.1002/(Sici)1097-0126(199905)48:5<346::Aid-Pi156>3.0.Co;2-N
4. Eds. L. Neufeld, F. Stassen, R. Sheppard, T. Gilman, The new plastics economy: Rethinking the future of plastics. *World Economic Forum* (2016). http://www3.weforum.org/docs/WEF_The_New_Plastics_Economy.pdf
5. T. Nimchua, H. Punnapayak, W. Zimmermann, Comparison of the hydrolysis of polyethylene terephthalate fibers by a hydrolase from *Fusarium oxysporum* LCH I and *Fusarium solani* f. sp. *pisi*. *Biotechnol. J.* **2**, 361-364 (2007). 10.1002/biot.200600095
6. T. Nimchua, D. E. Eveleigh, U. Sangwatanaroj, H. Punnapayak, Screening of tropical fungi producing polyethylene terephthalate-hydrolyzing enzyme for fabric modification. *J. Ind. Microbiol. Biot.* **35**, 843-850 (2008). 10.1007/s10295-008-0356-3
7. Materials and methods are available as supplementary materials on *Science* Online.
8. D. Ribitsch, E. H. Acero, K. Greimel, I. Eiteljoerg, E. Trotscha, G. Fredd, H. Schwab, G. M. Guebitz, Characterization of a new cutinase from *Thermobifida alba* for PET-surface hydrolysis. *Biocatal. Biotransform.* **30**, 2–9 (2012). doi:10.3109/10242422.2012.644435
9. W. Zimmermann, S. Billig, Enzymes for the biofunctionalization of poly(ethylene terephthalate). *Adv. Biochem. Eng. Biotechnol.* **125**, 97–120 (2011). doi:10.1007/10_2010_87
10. R. J. Müller, H. Schrader, J. Profe, K. Dresler, W. D. Deckwer, Enzymatic degradation of poly(ethylene terephthalate): Rapid hydrolyse using a hydrolase from *T. fusca*. *Macromol. Rapid Commun.* **26**, 1400–1405 (2005). doi:10.1002/marc.200500410
11. S. Sulaiman, S. Yamato, E. Kanaya, J. J. Kim, Y. Koga, K. Takano, S. Kanaya, Isolation of a novel cutinase homolog with polyethylene terephthalate-degrading activity from leaf-branch compost by using a metagenomic approach. *Appl. Environ. Microbiol.* **78**, 1556–1562 (2012). doi:10.1128/AEM.06725-11
12. C. M. Silva, F. Carneiro, A. O'Neill, L. P. Fonseca, J. S. M. Cabral, G. Guebitz, A. Cavaco-Paulo, Cutinase - A new tool for biomodification of synthetic fibers. *J. Polym. Sci. Part A: Polym. Chem.* **43**, 2448–2450 (2005). doi:10.1002/Pola.20684
13. M. A. M. E. Vertommen, V. A. Nierstrasz, M. van der Veer, M. M. C. G. Warmoeskerken, Enzymatic surface modification of poly(ethylene terephthalate). *J. Biotechnol.* **120**, 376–386 (2005). doi:10.1016/j.jbiotec.2005.06.015
14. E. Marten, R. J. Müller, W. D. Deckwer, Studies on the enzymatic hydrolysis of polyesters. II. Aliphatic-aromatic copolyesters. *Polym. Degrad. Stab.* **88**, 371–381 (2005). doi:10.1016/j.polymdegradstab.2004.12.001
15. K. Suzuki, A. Hori, K. Kawamoto, R. R. Thangudu, T. Ishida, K. Igarashi, M. Samejima, C. Yamada, T. Arakawa, T. Wakagi, T. Koseki, S. Fushinobu, Crystal structure of a feruloyl esterase belonging to the tannase family: a disulfide bond near a catalytic triad. *Proteins* **82**, 2857-2867 (2014). doi:10.1002/prot.24649

16. P. Kersey, L. Bower, L. Morris, A. Horne, R. Petryszak, C. Kanz, A. Kanapin, U. Das, K. Michoud, I. Phan, A. Gattiker, T. Kulikova, N. Faruque, K. Duggan, P. McLaren, B. Reimholz, L. Duret, S. Penel, I. Reuter, R. Apweiler, Integr8 and Genome Reviews: integrated views of complete genomes and proteomes. *Nucleic Acids Res.* **33**, D297–302 (2005). doi:10.1093/nar/gki039
17. M. Hosaka, N. Kamimura, S. Toribami, K. Mori, D. Kasai, M. Fukuda, E. Masai, Novel tripartite aromatic acid transporter essential for terephthalate uptake in *Comamonas* sp. strain E6. *Appl. Environ. Microbiol.* **79**, 6148–6155 (2013). doi:10.1128/AEM.01600-13
18. W. G. Cochran, Estimation of bacterial densities by means of the "most probable number". *Biometrics* **6**, 105–116 (1950). doi:10.2307/3001491
19. G. Muyzer, E. C. de Waal, A. G. Uitterlinden, Profiling of complex microbial populations by denaturing gradient gel electrophoresis analysis of polymerase chain reaction-amplified genes coding for 16S rRNA. *Appl. Environ. Microbiol.* **59**, 695–700 (1993).
20. R. K. Aziz, D. Bartels, A. A. Best, M. DeJongh, T. Disz, R. A. Edwards, K. Formsma, S. Gerdes, E. M. Glass, M. Kubal, F. Meyer, G. J. Olsen, R. Olson, A. L. Osterman, R. A. Overbeek, L. K. McNeil, D. Paarmann, T. Paczian, B. Parrello, G. D. Pusch, C. Reich, R. Stevens, O. Vassieva, V. Vonstein, A. Wilke, O. Zagnitko, The RAST Server: rapid annotations using subsystems technology. *BMC Genomics* **9**, 75 (2008). doi:10.1186/1471-2164-9-75
21. K. A. Baggerly, L. Deng, J. S. Morris, C. M. Aldaz, Differential expression in SAGE: accounting for normal between-library variation. *Bioinformatics* **19**, 1477-1483 (2003). doi:10.1093/bioinformatics/btg173
22. A. S. Juncker, H. Willenbrock, G. Von Heijne, S. Brunak, H. Nielsen, A. Krogh, Prediction of lipoprotein signal peptides in Gram-negative bacteria. *Protein Sci.* **12**, 1652-1662 (2003). doi:10.1110/ps.0303703
23. D. Ochoa, F. Pazos, Studying the co-evolution of protein families with the Mirrortree web server. *Bioinformatics* **26**, 1370–1371 (2010). doi:10.1093/bioinformatics/btq137
24. K. Tamura, G. Stecher, D. Peterson, A. Filipski, S. Kumar, MEGA6: Molecular evolutionary genetics analysis version 6.0. *Mol. Biol. Evol.* **30**, 2725–2729 (2013). doi:10.1093/molbev/mst197
25. M. Sasoh, E. Masai, S. Ishibashi, H. Hara, N. Kamimura, K. Miyauchi, M. Fukuda, Characterization of the terephthalate degradation genes of *Comamonas* sp. strain E6. *Appl. Environ. Microbiol.* **72**, 1825–1832 (2006). doi:10.1128/AEM.72.3.1825-1832.2006
26. H. Fujisawa, O. Hayaishi, Protocatechuate 3,4-dioxygenase. I. Crystallization and characterization. *J. Biol. Chem.* **243**, 2673-2681 (1968).
27. A. M. Orville, N. Elango, J. D. Lipscomb, D. H. Ohlendorf, Structures of competitive inhibitor complexes of protocatechuate 3,4-dioxygenase: multiple exogenous ligand binding orientations within the active site. *Biochemistry-Us* **36**, 10039-10051 (1997). doi:10.1021/bi970468n
28. C. Silva, S. Da, N. Silva, T. Matama, R. Araujo, M. Martins, S. Chen, J. Chen, J. Wu, M. Casal, A. Cavaco-Paulo, Engineered *Thermobifida fusca* cutinase with increased activity on polyester substrates. *Biotechnol. J.* **6**, 1230-1239 (2011). doi:10.1002/biot.201000391
29. A. Eberl, S. Heumann, T. Bruckner, R. Araujo, A. Cavaco-Paulo, F. Kaufmann, W. Kroutil, G. M. Guebitz, Enzymatic surface hydrolysis of poly(ethylene terephthalate) and

554 bis(benzoyloxyethyl) terephthalate by lipase and cutinase in the presence of surface
555 active molecules. *J. Biotechnol.* **143**, 207–212 (2009). doi:10.1016/j.jbiotec.2009.07.008
556 30. K. E. Griswold, N. A. Mahmood, B. L. Iverson, G. Georgiou, Effects of codon usage
557 versus putative 5'-mRNA structure on the expression of *Fusarium solani* cutinase in the
558 *Escherichia coli* cytoplasm. *Protein Expr. Purif.* **27**, 134-142 (2003). doi:10.1016/S1046-
559 5928(02)00578-8
560 31. A. M. Ronkvist, W. C. Xie, W. H. Lu, R. A. Gross, Cutinase-catalyzed hydrolysis of
561 poly(ethylene terephthalate). *Macromolecules* **42**, 5128–5138 (2009).
562 doi:10.1021/Ma9005318
563 32. E. H. Acero, D. Ribitsch, G. Steinkellner, K. Gruber, K. Greimel, I. Eiteljoerg, E.
564 Trotscha, R. Wei, W. Zimmermann, M. Zinn, A. Cavaco-Paulo, G. Freddi, H. Schwab, G.
565 Guebitz, Enzymatic surface hydrolysis of PET: Effect of structural diversity on kinetic
566 properties of cutinases from *Thermobifida*. *Macromolecules* **44**, 4632–4640 (2011). doi:
567 10.1021/Ma200949p
568 33. D. Ribitsch, E. H. Acero, K. Greimel, A. Dellacher, S. Zitzenbacher, A. Marold, R. D.
569 Rodriguez, G. Steinkellner, K. Gruber, H. Schwab, G. M. Guebitz, A new esterase from
570 *Thermobifida halotolerans* hydrolyses polyethylene terephthalate (PET) and polylactic
571 acid (PLA). *Polymers-Basel* **4**, 617-629 (2012). doi:10.3390/polym4010617
572 34. F. Kawai, M. Oda, T. Tamashiro, T. Waku, N. Tanaka, M. Yamamoto, H. Mizushima, T.
573 Miyakawa, M. Tanokura, A novel Ca^{2+}-activated, thermostabilized polyesterase capable
574 of hydrolyzing polyethylene terephthalate from *Saccharomonospora viridis* AHK190.
575 *Appl Microbiol Biot* **98**, 10053-10064 (2014). doi:10.1007/s00253-014-5860-y
576 35. D. Ribitsch, S. Heumann, E. Trotscha, E. Herrero Acero, K. Greimel, R. Leber, R.
577 Birner-Gruenberger, S. Deller, I. Eiteljoerg, P. Remler, T. Weber, P. Siegert, K. H.
578 Maurer, I. Donelli, G. Freddi, H. Schwab, G. M. Guebitz, Hydrolysis of
579 polyethyleneterephthalate by *p*-nitrobenzylesterase from *Bacillus subtilis*. *Biotechnol.*
580 *Prog.* **27**, 951–960 (2011). doi:10.1002/btpr.610
581 36. S. Chen, X. Tong, R. W. Woodard, G. Du, J. Wu, J. Chen, Identification and
582 characterization of bacterial cutinase. *J. Biol. Chem.* **283**, 25854-25862 (2008).
583 doi:10.1074/jbc.M800848200
584 37. T. Koseki, A. Hori, S. Seki, T. Murayama, Y. Shiono, Characterization of two distinct
585 feruloyl esterases, AoFaeB and AoFaeC, from *Aspergillus oryzae*. *Appl. Microbiol.*
586 *Biotechnol.* **83**, 689-696 (2009). doi:10.1007/s00253-009-1913-z
587 38. D. Pérez-Pantoja, R. Donoso, L. Agullo, M. Cordova, M. Seeger, D. H. Pieper, B.
588 Gonzalez, Genomic analysis of the potential for aromatic compounds biodegradation in
589 *Burkholderiales*. *Environ. Microbiol.* **14**, 1091–1117 (2012). doi:10.1111/j.1462-
590 2920.2011.02613.x
591 39. N. Kamimura, T. Aoyama, R. Yoshida, K. Takahashi, D. Kasai, T. Abe, K. Mase, Y.
592 Katayama, M. Fukuda, E. Masai, Characterization of the protocatechuate 4,5-cleavage
593 pathway operon in *Comamonas* sp. strain E6 and discovery of a novel pathway gene.
594 *Appl. Environ. Microbiol.* **76**, 8093–8101 (2010). doi:10.1128/AEM.01863-10

595